



BRNO UNIVERSITY OF TECHNOLOGY

VYSOKÉ UČENÍ TECHNICKÉ V BRNĚ

FACULTY OF MECHANICAL ENGINEERING

FAKULTA STROJNÍHO INŽENÝRSTVÍ

INSTITUTE OF MANUFACTURING TECHNOLOGY

ÚSTAV STROJÍRENSKÉ TECHNOLOGIE

FRICTION WELDING OF MATERIALS

FRIKČNÍ SVAŘOVÁNÍ MATERIÁLŮ

BACHELOR'S THESIS

BAKALÁŘSKÁ PRÁCE

AUTHOR

AUTOR PRÁCE

Daniel Chrást

SUPERVISOR

VEDOUCÍ PRÁCE

doc. RNDr. Libor Mrňa, Ph.D.

BRNO 2021

Assignment Bachelor's Thesis

Institut: Institute of Manufacturing Technology
Student: **Daniel Chrást**
Degree program: Engineering
Branch: Manufacturing Technology
Supervisor: **doc. RNDr. Libor Mrňa, Ph.D.**
Academic year: 2020/21

As provided for by the Act No. 111/98 Coll. on higher education institutions and the BUT Study and Examination Regulations, the director of the Institute hereby assigns the following topic of Bachelor's Thesis:

Friction welding of materials

Brief Description:

Acquainted with friction welding technology. Principles, equipment, advantages and disadvantages.

Bachelor's Thesis goals:

Acquire the technology of friction welding, develop research and the possibilities of this technology and its current use in industry.

Recommended bibliography:

MORAVEC J.: Teorie svařování a pájení II - Speciální metody svařování, TUL, 2008, 150 str., ISBN 978-80-7372.

KANNATEY-ASIBU, E.: Principles of Materials Processing, John Wiley&Sons, Inc. Publication, 2009, ISBN 978-0-470-17798-3.

AMBROŽ O., KANDUS B., KUBÍČEK J.: Technologie svařování a zařízení, Ostrava, Zeross, 2001, 395 str. ISBN 80-85771-81-0.

Deadline for submission Bachelor's Thesis is given by the Schedule of the Academic year 2020/21

In Brno,

L. S.

doc. Ing. Petr Blecha, Ph.D.
Director of the Institute

doc. Ing. Jaroslav Katolický, Ph.D.
FME dean

ABSTRACT

CHRÁST Daniel: Friction welding of materials.

The work deals with the examination of welds made of AISI 316L and TI GR2 materials. These welds were formed by rotary friction welding. The first part of the work consists of a literature review and state of the art of rotary friction welding state of the art. The second part of the work presents the results of welded joints examination. The macrostructure, microstructure, microhardness in all areas of the welded joint was examined, the materials passed the test of chemical composition and the welded joint was subjected to a tensile test.

Keywords: rotational friction welding, AISI 316L, TI GR2

ABSTRAKT

CHRÁST Daniel: Frikční svařování materiálů.

Práce se zabývá zkoumáním svárů z materiálů AISI 316L a TI GR2. Svár je zhotovený rotačním třecím svařováním. První část práce je literární rešerše na téma rotačního svařování třením. V druhé části práce jsou uvedeny výsledky zkoumání svařovaných spojů. Byla zkoumána jejich makrostruktura, mikrostruktura, mikrotvrdost ve všech oblastech svarového spoje, materiály prošly zkouškou chemického složení a svarový spoj byl vystaven tahové zkoušce.

Klíčová slova: rotační svařování třením, AISI 316L, TI GR2

BIBLIOGRAPHY

CHRÁST, Daniel. *Frikční svařování materiálů* [online]. Brno, 2021 [cit. 2021-03-21]. Dostupné z: <https://www.vutbr.cz/studenti/zav-prace/detail/132814>. Bakalářská práce. Vysoké učení technické v Brně, Fakulta strojního inženýrství, Ústav strojírenské technologie. Vedoucí práce Libor Mrňa.

AFFIDATIV

I declare that I have elaborated my bachelor thesis on the theme of “Friction welding of materials” independently with the use of technical literature and other sources quoted throughout thesis and detailed at the end in list of literature.

.....
Date

.....
Daniel Chrást

ACKNOWLEDGEMENT

I would like to thank doc. RNDr. Libor Mrňa Ph.D. for valuable comments and advice regarding the elaboration of the bachelor's thesis. Representatives of Tecpa s.r.o for the possibility of processing a bachelor's thesis and professional consultation. Ing. Kamil Podaný Ph.D. for assistance in design the tensile test. I would also like to thank my girlfriend, family and especially my brother Mgr. Petr Chrást Ph.D. for language proofreading of the bachelor's thesis and my father Pavel Chrást for his help with welding.

1 TABLE OF CONTENTS

| | |
|------------------------|--|
| ABSTRACT | |
| BIBLIOGRAPHIC CITATION | |
| AFFIDAVIT | |
| ACKNOWLEDGMENT | |
| CONTENT | |
| TABLE OF CONTENTS | |

| | |
|---|----|
| INTRODUCTION | 10 |
| 1 ANALYSIS OF THE EXPERIMENT [1] [2] | 11 |
| 2 FRICTION WELDING TECHNOLOGY | 12 |
| 2.1 Introduction [3] [4] [5] | 12 |
| 2.2 History [3] [6] [7] | 12 |
| 2.3 Types of friction welding [3] [4] [8] | 12 |
| 2.4 Principle of friction welding [3] [4] [6]..... | 13 |
| 2.5 The process of friction welding [3] [4] [6] [10] | 14 |
| 2.6 Parameters of friction welding [5] [6] [7] [10] [11] | 15 |
| 2.6.1 Coefficient of friction [3] [4] [11]..... | 16 |
| 2.6.2 Temperature [12] [13] | 17 |
| 2.7 Friction welding at low pressure and temperature [14] [15] [16] | 18 |
| 2.8 Preparation and surface treatment of welded materials [3] [10] [13]..... | 19 |
| 2.9 Friction weldability of materials [3] [4] [11] | 20 |
| 2.10 Areas of weld [3] [13] [9] | 21 |
| 2.11 Heat treatment and defects of welded joints [3] [6] [10] | 22 |
| 2.12 Friction welding machines [3] [18] | 23 |
| 2.13 Use of friction welding in practice [3] [6] [13] | 24 |
| 2.14 Advantages and disadvantages of friction welding [4] [10] [11] [13]..... | 25 |
| 3 TESTS OF ROTATION FRICTION WELDS | 26 |
| 3.1 Destructive testing of welds | 26 |
| 3.1.1 Tensile test [3] [21] | 26 |
| 3.1.2 Charpy impact test [3] [21] | 26 |
| 3.1.3 Bending test [3] [21] | 26 |
| 3.1.4 Hardness test [3] [21] | 26 |
| 3.2 Metallographic tests of welds | 27 |
| 3.2.1 Macrostructure | 27 |
| 3.2.2 Microstructure | 27 |
| 3.3 Tensile tests of friction welded joints..... | 28 |
| 3.4 Sample preparation | 29 |
| 3.5 Non-destructive weld testing | 31 |
| 3.5.1 Visual test [3] [5] [10]..... | 31 |
| 3.5.2 Penetrative test [3] [5] [10] | 31 |
| 3.5.3 Magnetic powder test [3] [5] [10] | 31 |
| 3.5.4 Ultrasonic test [3] [5] [10]..... | 31 |
| 3.5.5 Radiation test [3] [5] [10]..... | 31 |
| 4 WELDED MATERIALS | 32 |
| 4.1 Steel AISI 316L [22] [23] [24] | 32 |
| 4.2 Titanium Ti GR 2 [26] [27] [25] | 32 |
| 5 DESIGN AND EXECUTION OF THE EXPERIMENT | 33 |
| 5.1 Production of semi-finished products for rotary friction welding..... | 33 |
| 5.2 Welding process | 34 |

| | | |
|-------|--|----|
| 5.2.1 | Welding process of AISI 316L and Ti GR2..... | 34 |
| 5.2.2 | Welding process of AISI 316L | 36 |
| 5.2.3 | Welding process of Ti GR 2..... | 36 |
| 5.3 | Evaluation of macrostructure | 37 |
| 5.4 | Evaluation of microstructure | 38 |
| 5.5 | Execution and evaluation of tensile test | 39 |
| 6 | CONCLUSIONS | 42 |

BIBLIOGRAPHY

TABLE OF SYMBOLS AND ABBREVIATION

TABLE OF FIGURES

TABLE OF FORMULAS

TABLE OF CHARTS

TABLE OF GRAPHS

TABLE OF ATTACHMENT

INTRODUCTION

The inseparable connection of materials is a current industrial issue. The growth of global competition and global technological progress provide increasingly modern methods for joining materials. In the process of welding, two identical as well as different materials are connected. The most common welding method is fusion methods, which are used for a wide range of applications. These include TIG, MAG, MIG welding, laser and plasma welding. Other methods use pressure to generate heat in the weld. These methods include resistance welding or friction welding. Although fusion methods are the most widely used, they are not universal and may in some cases be replaced by other methods, such as friction welding, where it can produce certain types of welds cheaper, faster and with better quality.

Friction welding is one of the most prominent welding methods with increasing popularity. It offers many advantages for joining materials, compared to other methods. The individual chapters will focus on the description of the experiment in the connection of two heterogeneous metals in the company Tecpa s.r.o., which deals with the production of precise and complex components. The focus of this thesis is to explore a methodical approach for joining X2CrNiMo17-12-2 and TI GR2 alloys for potential industrial applications.

1 ANALYSIS OF THE EXPERIMENT [1] [2]

This thesis deals with joining of heterogeneous materials using friction welding. In the experiment, joining of stainless steel and titanium surfaces will be attempted via rotary friction welding. The results will be further analysed in both microscopic and macroscopic scale as well as with mechanical testing of tensile strength of the joints. The goal is to determine whether these two alloys are weldable at such efficiency that this methodics could be introduced into industrial processes. The task is therefore also to find out possibilities of input parameter optimization to improve the quality of the connection.

The work describes an experiment dealing with the connection of two heterogeneous materials X2CrNiMo17-12-2 and TI GR2. The company Tecpa s.r.o. intends to manufacture rods and pipes via rotary friction welding and it is therefore vital to find out given parameters, which would provide sufficiently high-quality connection of both materials that can be subsequently introduced into operation.

Under experimental conditions $\varnothing 10$ mm bars made of X2CrNiMo17-12-2 and TI GR2 were joined. Welding parameters such as speed, pressure, or pre-heating conditions were optimised. Welding was performed at Pavel Chrást metalworks on a conventional lathe.

2 FRICTION WELDING TECHNOLOGY

2.1 Introduction [3] [4] [5]

Friction welding is classified as a method of pressure welding. The principle is based on simultaneous rotational movement of two components, where their surfaces chafe against each other under pressure until the material surfaces start to melt, and subsequent compression, which forms the weld between the two surfaces. The greatest use is in joining components of cylindrical shapes such as shafts or tubes. However, it is also possible to combine parts of different shapes, the only requirement are two parallel surfaces. This welding process does not require any additional material to form a weld. The formation of a weld is achieved with the help of plastic deformation, which is supported by axial pressure and local heating. Heat is generated due to friction between the two surfaces. Elevated temperature occurs predominantly in the narrow range between welded surfaces and reaches values of 0.8 – 0.85 % of the melting temperature of the base material. In the case of steel, this temperature is around 1200–1300 °C. Friction welding yields high quality welds with a small heat affected zone and very good mechanical properties, even comparable to the properties of the base material.

2.2 History [3] [6] [7]

Friction welding dates back to the beginning of 20th, when it was patented by A. I. Chudikov in USSR, for rotary welding of flexible rods. The method was further developed and between 1920 and 1944, several patents were issued in Europe, but did not find much use. After the WWII, it proved successful in welding of thermoplastic pipes. A greater development took started after the publication of A. I. Chudikov's patent in 1956. In 1957, first welding machine was built in Czechoslovakia by modifying a turret lathe for research purposes. Other machines were successfully tested in factories, thanks to good quality of welds and a good economic aspects of production of welds, more and more friction machines were involved in to normal production. Furthermore, there was an effort for welding of non-rotating parts and non-rotating shape. Orbital friction welding began to be applied in the 1970s and subsequently in the 1980s. years of linear friction welding.

2.3 Types of friction welding [3] [4] [8]

In the beginning, mostly rotary parts were welded, mainly due to the fact that mostly conventional lathes were used for this purpose. There have been requirements for welding shapes other than only rotary. The friction process can be further divided, as seen in Fig. 1:

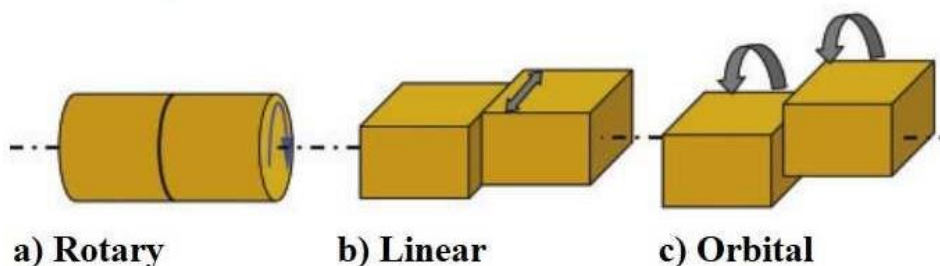


Fig. 1 types of friction welding process [9]

2.4 Principle of friction welding [3] [4] [6]

Theoretically, if it was possible to attach two single crystals that have completely flat and clean contact surfaces and it could press them together to the distance of the crystal lattice plane, the connection would be formed due to interatomic forces without external forces and at any temperature. In reality, the real material is not formed by one large crystal but consists of many small, interconnected crystals. They are also not perfectly straight and clean. It has been used for external pressure for welding, to increase the forces and temperatures at the point of contact.

Friction joining of two surfaces has a molecular and mechanical character. Molecular indicates being caused by the mutual interaction of atoms, and mechanical being the process of surface interfacing. It is not known if it is more important for the joining of materials diffusion or mechanical mixing of the two welded materials (see Fig. 2). Due to the increased temperature at the contact planes of welded materials, diffusion is considered a driving mechanism. It has been supported by cleaning processes caused by

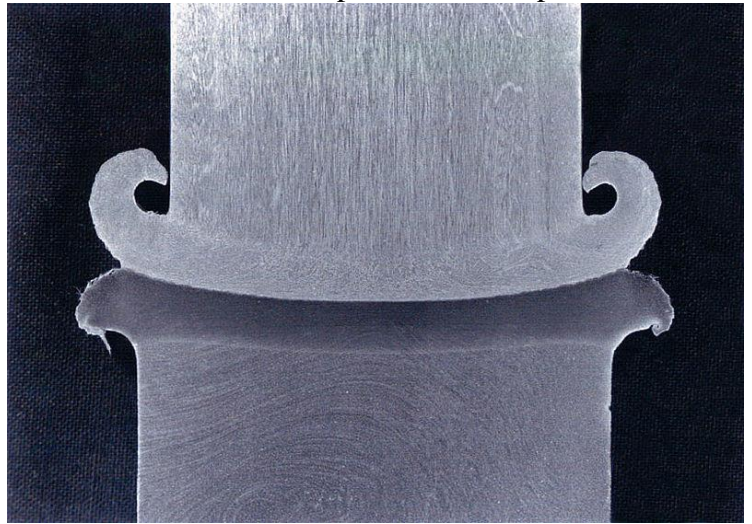


Fig. 2 diffusion of friction welding materials [28]

simultaneous movement and pressing of both components. When two planes of identical chemical composition are connected via friction welding the diffusion driven process is balanced which results in a high-quality weld. However, when welding materials of different chemical composition, it may have diffusion good and bad effect on the welded joint. For example, when welding two large steels the difference in carbon content causes decarburization of the steel with a higher C content, which can cause increase the ductility of the weld. On the other hand, for example, when welding steel with aluminium, copper, or titanium, intermetallic and hard phases can form, which results in brittle welds. Literature based research excludes diffusion as the primary mechanism of weld formation, based on a very sharp transition, for example in the joint between titanium and aluminium, or various titanium alloys (see Fig. 3). When a welded junction of two different titanium alloys was analysed, it was found that due to the fast temperature cycle low diffusivity of materials was shown and rather the formation of the joint was attributed to mutual mechanical stir in a narrow zone around the weld.

2.5 The process of friction welding [3] [4] [6] [10]

Prior to welding, surfaces should be cleaned, free of slag oxides and grease. Roughness does not have a great influence on the process. Components are most often modified by turning, milling, cutting or shearing. The procedure for rotation friction welding can generally be divided into several steps:

The first step is clamping welded parts. It must be solid and accurate, therefore for clamping tools are designed for various shapes of connected parts. The tools must be durable enough to withstand the pressures applied and heat.

The clamped parts are then set to the desired relative position as they will be connected. Welded surfaces are brought together. One part is moved and there is a slight pressure applied between the two planes.

When full speed is achieved, the frictional contact force increases to the required value, which simultaneously with the rotation leads to increase in the temperature between the planes. The results in the plasticization of the material and its gradual extrusion into the burr. The friction movement is stopped after shortening of the component, certain time period or exact rotation count.

Cessation of welding is a rapid process, and a part must be stopped in the final position for welding. The forging force is applied to form a weld.

The last step is to release the forging force and remove the connected parts.

Process can be divided into four phases, as it can be seen in Fig. 3

- Phase a) - The first contact of moving parts comes into contact only peaks of inequality. Due to dry friction, the temperature at the point of contact increases and gradually there is also the surface abrade and the contact area increases. There is no mixing or significant shortening of the component.

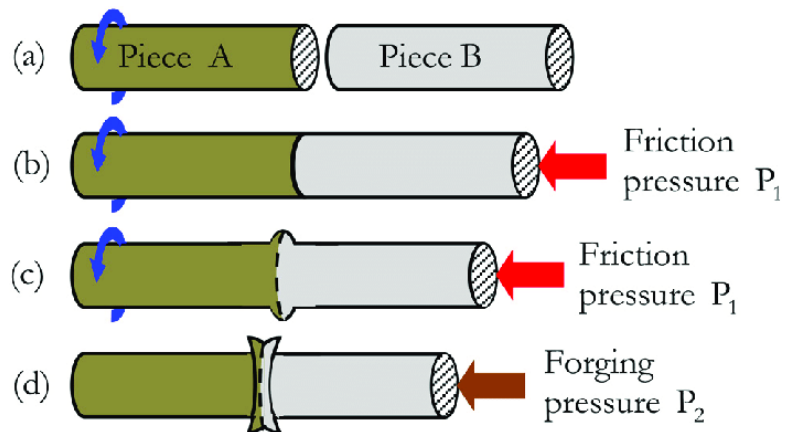


Fig. 3 Phases of friction welding process [29]

- Phase b) - The temperature between the surfaces continues to rise and the material is plasticized. Materials are less able to withstand the applied force.

- Phase c) - Material is precipitated into the burr, which leads to shortening of the part.

- Phase d) - The movement is stopped, and a forging force is applied.

2.6 Parameters of friction welding [5] [6] [7] [10] [11]

The welding process is affected by several parameters that enter the welding process. The waveforms are shown in Figure 4. Parameters such as rotational speed, specific pressure, temperature, and overall shortening were used.

Rotation speed expresses the number of revolutions per minute [rpm]. In practice, they are chosen within wide limits, as it distinguishes between values for ferrous and non-ferrous materials. The most used relationships for calculating the rotational speed can be seen in the samples, where d is the diameter of the welded part in millimetres and n is the revolutions per minute.

$$\text{steel: } n \cdot d = (1,2 \div 6,0) \cdot 10^4 [\text{rpm}] \quad (2.6.1)$$

$$\text{copper: } n \cdot d = (4,0 \div 4,5) \cdot 10^4 [\text{rpm}] \quad (2.6.2)$$

$$\text{titanium: } n \cdot d = (8,0 \div 10) \cdot 10^4 [\text{rpm}] \quad (2.6.3)$$

The specific pressure is one of the most important welding parameters, as it affects the generation of heat on the contact surfaces and determines the required power input of the welding machine. Two types of welding pressures are distinguished.

The magnitude of the specific friction pressure affects the heating rate of the welded parts, the loss of material and the magnitude of the friction torque. The magnitude of the specific friction pressure is in the range of $10 \div 80$ MPa. The application period of the specific friction pressure is relative, as it is necessary to achieve sufficient melting of the materials on the contact surfaces.

The size of the forging pressure affects the quality of the welded joint. It is important that it takes place when the relative movement is stopped, otherwise the strength of the joint is reduced. The magnitude of the specific forging pressure is twice the specific friction pressure and varies in values $20 \div 150$ MPa. The action time of the specific forging pressure ranges from $0 \div 3$ seconds.

These parameters can be used for single-purpose machines designed for a given technology. In case, when lathe has been used, it uses the feed of the static part for the rotating at a constant feed, to create the same specific pressure. It uses the movement of the quill as such a piston to push the materials into each other.

To create a quality weld, it is necessary to bring enough heat to the weld. The heat generated is directly dependent on the speed of rotation and the specific pressure used in welding. The size of these parameters can be combined to achieve the best welding conditions. For example, by increasing the rotational

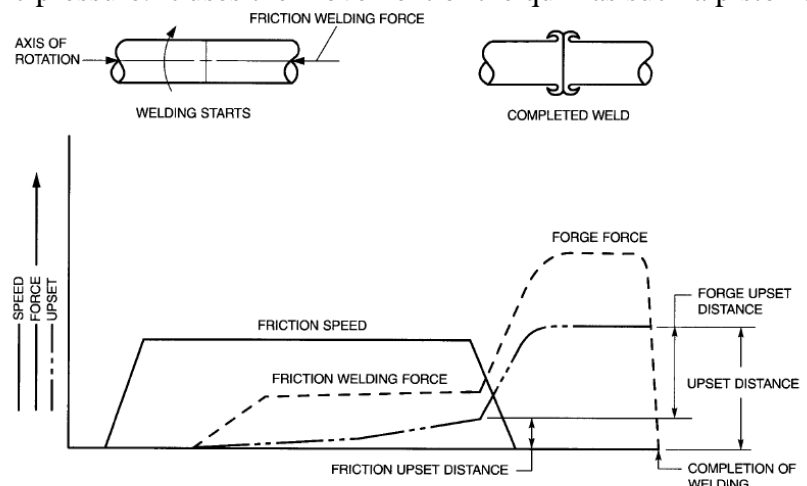


Fig. 4 friction welding parameters [30]

speed, it is possible to reduce the specific pressure. This can be used for components that do not have an ideal construction and could be deformed, or, for example, to create a joint with better mechanical properties.

Overall shortening is one of the disadvantages of friction welding. Since the individual materials and their surfaces are melted and subsequently compressed and the neck is formed,

2.6.1 Coefficient of friction [3] [4] [11]

The coefficient of friction is an important parameter that numerically characterizes the frictional resistance of the surfaces a pair of bodies of different materials (in Fig 5). It is a scalar. This is further divided into static coefficient of friction and dynamic coefficient of friction. it is denoted by f or μ . The static or dynamic coefficient of friction is denoted by μ_s resp. μ_d . The static coefficient of friction is usually greater and expresses the resistance that the body withstands under the force just before the body is set in motion. Dynamic coefficient of friction usually reaches smaller values and the action of forces on the body during its movement is obtained. The size of the friction force, depends on the speed, contact pressure, temperature, and roughness of the friction surfaces. The coefficient of friction is a quantity equal to the ratio of tangential force of friction to the perpendicular compressive force (at a constant surface area).

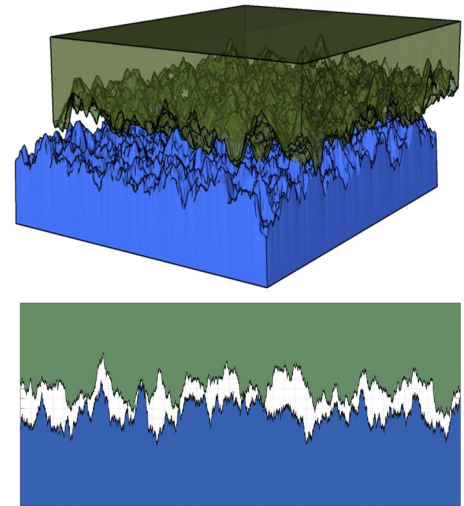


Fig. 5 real surface of two bodies [31]

$$f = \frac{\bar{\tau}}{\bar{\sigma}} \quad (2.6.4)$$

The magnitude of the coefficient of friction is generally not a constant value and depends on many parameters such as the cleanliness and condition of the surface, its geometry, the properties of the materials and finally on the friction process, such as pressure, relative velocity, or temperature. Metal oxide layers are always harder than the base material. If the layers are thick, the value increase the coefficient. As shown on Table 1 the examples of coefficients friction of materials with and without oxide layer are different. The coefficient also changes proportionally with speed movement, individual waveforms are shown in Fig. 6

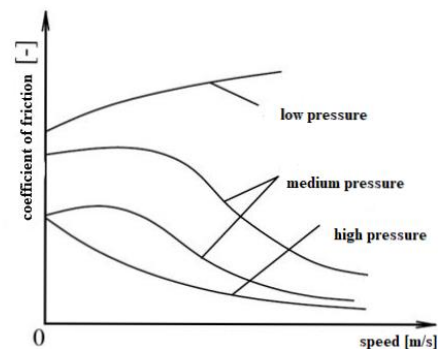


Fig. 6 coefficient of friction [32]

Chart 1 Coefficients of friction of materials [3]

| | metal | Au | Ag | Sn | Al | Zn | Cu | Fe | Cr | Ti |
|---------|----------------|----|-----|----|-----|-----|-----|-----|-----|-----|
| Surface | Oxidised | - | 0,6 | 1 | 0,8 | 1,2 | 0,6 | 1 | 0,4 | 0,4 |
| | Metallic clean | 2 | 1 | 1 | 1,2 | 0,8 | 1,6 | 0,6 | - | 0,3 |

2.6.2 Temperature [12] [13]

Heat between materials is released due to friction but can also be introduced by an external thermal source. During the process, the material must be optimally plasticized and be partially extruded into the burr. The greatest friction, and the development the heat occurs on the edge and decreases towards the middle. The advantage of friction welding over arc methods is relatively small heat input to material and thus a significantly smaller heat-affected area around the weld. Size comparison of heat-affected areas with arc methods are shown in the diagrams in Fig. 7 and Fig. 8.

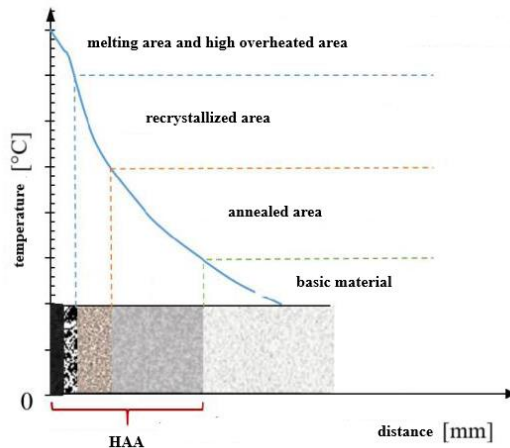


Fig. 7 heat-affected area of arc methods [6]

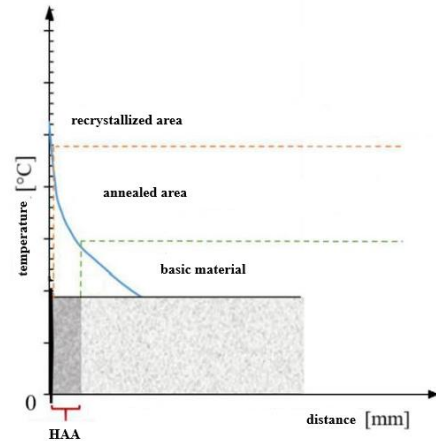


Fig. 8 heat affected area of friction welding [6]

Friction welding does not burn the alloying elements and in some cases the weld location cannot be identified after the normalization annealing. The structural properties tend to be very good for mixed welded joints, as metals do not melt during friction welding and no hot cracks are formed in welds when mixed. Furthermore, no soft intermediate phases are formed in the weld joint, and it is possible to weld almost any materials without defects.

When friction welding of steels, the components have a temperature higher than the transformation temperature A_3 for sub-eutectoid steels and A_{Cm} for super-eutectoid steels. Welding takes place in the austenite region and therefore the material does not melt. The depth of the austenitic zone depends on the welding parameters, but mainly on the chemical composition of the materials. In the case of steels, the austenitic zone is followed by another temperature range A_1 and A_3 . The structure is formed by austenite and ferrite in sub-eutectoid steels. In super-eutectoid steels, the structure consists of austenite and cementite. The size of the parameters has a fundamental effect on the growth of austenitic grain, because it reaches the critical temperature range, especially when welding steels with a higher carbon content in the structure. The advantage of friction welding is deformation during the application of specific friction pressure, as this causes deformation and thus reduces grain coarsening. The specific forging pressure has a final effect on the austenitic grain since the final size of the austenitic grain after forming depends on the amount of deformation and the temperature.

As the temperature is not constant throughout the volume of materials to be welded, cold forming can occur in some places, especially for materials with low thermal conductivity. Rapid heat dissipation from the weld site causes partial turbidity. This results in increased hardness at the weld site. Depending on the type of material, a martensitic structure may appear in the structure, which must then be removed by further heat treatment.

2.7 Friction welding at low pressure and temperature [14] [15] [16]

Friction welding under reduced pressure is an adjustment of specific friction pressure, which expands the possibilities of welding. This method combines friction welding with diffusion welding. During the process, the use of an external heat source is used to assist during heating of the components, which allows for less specific frictional pressure to be applied and for decreasing of the time required for heating. This adjustment of the parameters offers several advantages, including the reduction of the protrusion while maintaining the same quality of the welded joint, since the cleaning processes are not eliminated. This modification also allows us to weld materials and components that cannot be welded under normal conditions due to too large a contact area for which the specific friction pressure is not sufficient to create a sufficient temperature. It is also possible to reduce the heat affected zone. Thanks to the use of an external heating device, it is possible to use smaller machines, as it is not necessary to develop such a high specific friction pressure. In addition, it is possible to weld components with a larger welded area on a smaller machine. The last advantage is the reduction of welding times, since the time for heating of the contact surfaces is decreased as well as material losses during heating. The technology of low-temperature friction welding and the modification of friction welding is applicable especially to steels. When welding steels by conventional friction welding, the materials do not melt, but they are heated to a temperature of up to 80 ÷ 85% of the melting temperature, it is a temperature of approximately 1200 °C. Such a temperature corresponds to heating in the austenite region. After cooling, a hard martensitic structure often occurs in the welds, but this is undesirable in most cases. The martensitic structure can be prevented by a lower heating temperature, and therefore the resulting temperature must be below the recrystallization temperature. As mentioned earlier, the temperature is most affected by the rotational speed, the specific friction pressure, or by an external heating source. Reducing the temperature and at the same time maintaining the quality of the welded joint can be achieved by reducing the speed of rotation and a significant increase in the pressing force. The distribution of friction welding by temperature has been shown in figure 9.

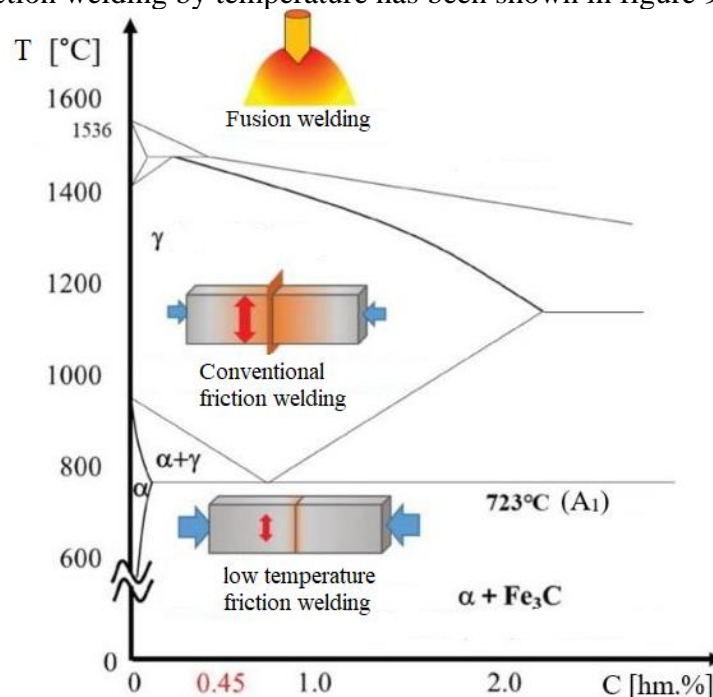


Fig. 9 Low temperature welding in Fe-Fe₃C diagram [16]

2.8 Preparation and surface treatment of welded materials [3] [10] [13]

The disadvantage of rotary friction welding is that one of the welded parts must rotate. Therefore, this method is particularly suitable for welding of rotating parts, but the static part does not have to have a circular shape, it depends mainly on the clamping. The basic shapes of the connected parts include rods, tubes, pins, and further shaped parts. It must follow the rule that it clamps a part with a larger moment of inertia in a rotating position.

The preparation of parts with different cross-sectional sizes for welding depends on the quality of the materials and the resulting use of the joint; for example, in some cases the burr caused by welding may not be removed. It is important to make sure that the unloading of the parts from the clamping elements is as small as possible. This increases the rigidity of the parts during welding and reduces the magnitude of vibrations that could create misalignment or other disbalances in the welded joint. For welding materials with high thermal conductivity, an unloading of more than $0.75 \cdot d$ is recommended. Conversely, for materials with low thermal conductivity, a lining of $0.5 \cdot d$ is recommended. If a larger lining of materials was required, but there would be a reduction in rigidity, then the contact surfaces have to be adjusted, as shown in the figure 10.

If heterogeneous materials have to be connected via by friction welding, there are problems associated with different physical and mechanical properties of individual materials. Different thermal conductivities and strengths at higher temperatures lead to different degrees of plastic deformation. Some materials do not deform at all. To create a quality joint, it is necessary to ensure symmetrical clamping of both welded materials. In case of materials that have lower strengths under high temperatures, it undergoes greater plastic deformation and is intensively extruded into burrs. There is not enough contact of materials around the circuit and thus there will be no connection. This problem can be solved as follows:

- Choosing the diameter of the part made of softer material by 15 ÷ 25% larger.
- Applying a special surface treatment adjustment, see figure 10.
- Preheating of a part made of stronger material before welding
- Using a support preparation for a softer material
- Regulating the pressure program during welding

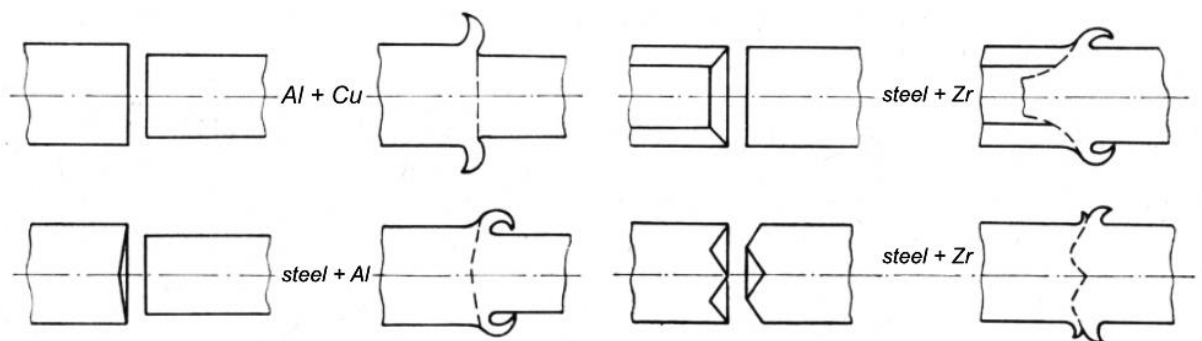


Fig. 10 Preparation and surface treatment [3]

2.9 Friction weldability of materials [3] [4] [11]

Friction welding technology offers many material combinations to connect. Weldability depends mainly on the chemical composition of the material, physical properties, geometry and cross-sectional size of welded parts and welding parameters. Friction welding is not significantly sensitive to differences in the chemical composition of the joined materials. Various combinations of material can be combined, which cannot be combined by other methods. This is especially true for materials with very different melting temperatures, chemical composition, and type of microstructure. It is possible to weld ferrous and non-ferrous metals, plastics and, under certain conditions, ceramics, or glass. Among the well weldable materials are steel, aluminium, copper, nickel, molybdenum, titanium, then aluminium alloyed with various metals such as zirconium, tungsten, titanium, nickel, magnesium, copper, and carbon steel.

Today, mostly titanium and nickel alloys are welded with this method. Figure 11 shows known combinations of weldable materials. Thanks to the principle of welding and the temperature below melting point they have a fine grain (10x to 30x compared to the base material) and no defects such as burns, hot cracks and gas cavities. On the contrary, in the case of a poorly performed forging phase, Cold joints or cold cracks can be formed. The welding processes nowadays are mostly automated, as a result, the reproducibility of the welds is good, they are suitable for both static and dynamic loaded components.

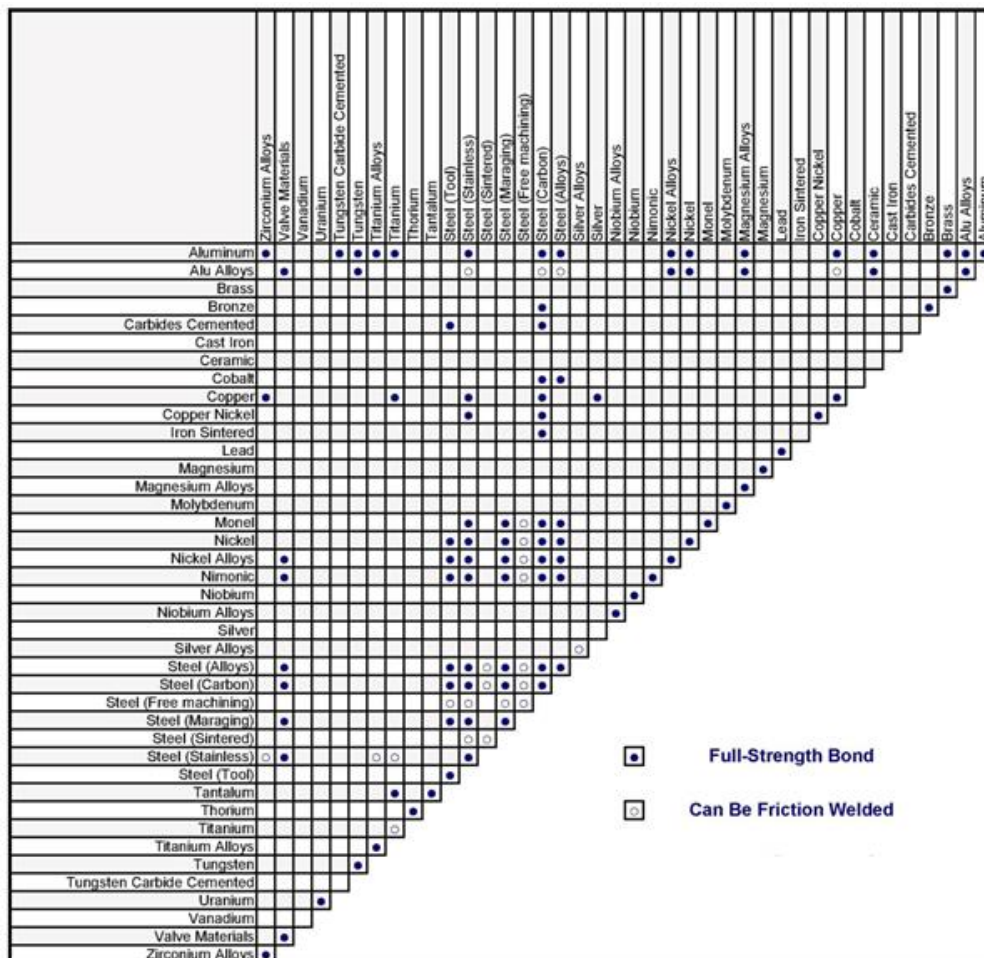


Fig. 11 Weldability of materials [17]

2.10 Areas of weld [3] [13] [9]

During friction welding, the joined components are affected not only thermally, but to a large extent also mechanically. The individual areas of the welded area are shown in fig 12

- I) plastic affected area of weld
- II) central area of weld
- III) thermally and mechanically affected area
- IV) thermally affected area
- V) basic material

The thermo-mechanically affected areas of the weld can be further divided by size plastic deformations; these are shown in more detail in Fig. 13.

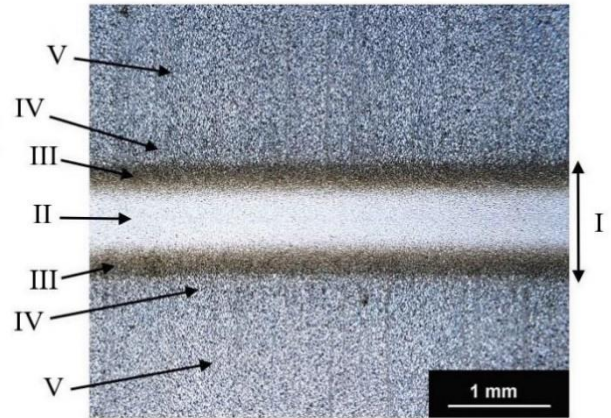


Fig. 12 friction welded areas [33]

- Area I is called the contact zone. Friction and mixing occur in this zone both materials that are significantly plastically deformed. The structure here is characterized by a very fine grain due to mechanical stress and complete recrystallization.

- Area II is called the fully plasticized zone. This is again significantly affected by plastic deformation, but no longer involved in frictional contact and mixing of the material. Plastic deformation together with high temperature leads to dynamic recrystallization, the grain in this This area is homogenous.

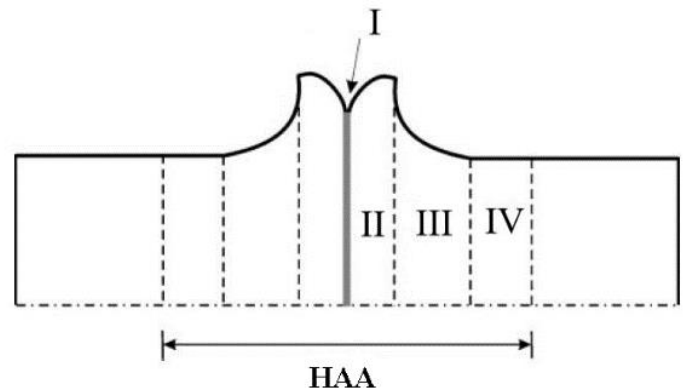


Fig. 13 Individual areas of friction weld [9]

- Area III is called a partially deformed zone. The degree of plastic deformation and temperature is lower here than in previously mentioned areas. As a result, there is a slight increase in grain size.

- Area IV is called the undeformed zone and is the furthest area from the weld within thermally affected areas. There is no longer any plastic deformation, and the zone is affected only thermally. As a result, the grain size may increase.

2.11 Heat treatment and defects of welded joints [3] [6] [10]

Not all welded joints need to be subjected to heat treatment and even if it's the case, the heat treatment has to be limited to the necessary minimum for economic as well as technological reasons. Each material responds to heat treatment in a different way.

In friction welding, there is a problem in the heat treatment of the welded joint. It requires various heat steps for welding heterogeneous materials.

In case of steels, heat treatment parameters are set easier than in heterogeneous materials. However, if the weld is made by ferrous and non-ferrous materials, it gets to the point where certain heat treatment values are set for the first material but are unsuitable for the second material.

One of the possibilities is to include heat treatment before welding is when the structure and properties of materials need to be adjusted to make them more weldable. The type of heat treatment is determined by the type of steel or the given material. If it is possible to apply heat treatment after welding, the main task is to reduce internal stress afterwards to improve the microstructure in HAZ and weld metal.

Because the friction weld is formed at temperatures below the liquidus curve, it eliminates several types of weld defects that occur with conventional welding methods, such as spatial defects including bubbles, inflammations, stalactites, or inclusions.

Other types of weld defects can be formed such as cracks, microcracks and non-penetrations as it can be seen in fig. 14 These defects result in causing high internal stresses and strains. If the defects occur in a welded joint, they can be assessed according to the subcritical size of surface defects. It is known that the degree of fatigue failure or brittle fracture failure is directly affected by these defects.

Since cracks are one of the most dangerous types of weld defects, it is important to eliminate them as much as possible. It can be achieved by adjusting welding parameters such as speed or specific friction pressure, or by heat treating materials to change their properties.

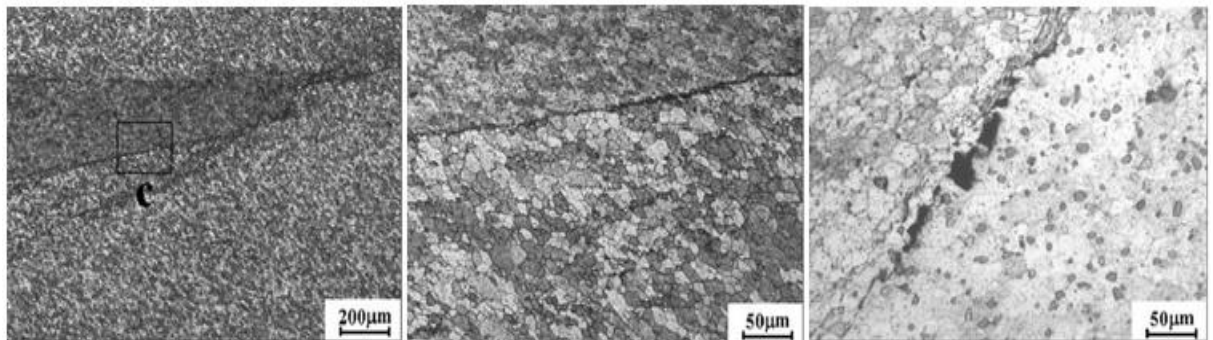


Fig. 14 Cracks in friction welds [45]

2.12 Friction welding machines [3] [18]

In general, the first experiments of rotary friction welding were performed on lathes and drills, as well as in the present experiment. It soon became apparent that these machines were not suitable for more complex joints such as bearings, spindles and frames, which were easily deformed by axial pressures and did not achieve the required rigidity to achieve an accurate final weld.

In particular, the required forging part of the welding of the heated contact surfaces requires a special construction of the moving parts. Furthermore, it was necessary to automate the welding process to achieve good economic results.

The basic principle of rotary friction welding can be achieved in various ways. Today, the two most common types are conventional and flywheel.

The principle of conventional welding is the same, it differs only in the design options of the welding machine. The motor drives a chuck in which the rotating welded part is clamped. The second part is clamped on the sliding support and is pressed against the rotating part by means of a piston as it can be seen on Fig 15.

Older methods did not use a brake to stop, but to allow the static component to be clamped. Newer methods use the brake to stop the rotation quickly. This method is used for machines that do not achieve such power of electric motors.

Flywheel friction welding is a more recent approach to friction welding. The kinetic energy caused by the rotation is transferred to the flywheel. Then the connection between the flywheel and the motor is broken and the kinetic energy is used to heat the components. This method of rotary friction welding does not require special braking devices. The amount of kinetic energy can be regulated by changing the speed or the weight of the flywheel. Two methods of flywheel friction welding are utilized. The first is utilizing all the energy of the flywheel. It is a very simple method, the instrument is less sensitive to failures, has a longer service life and better use of kinetic energy. The second method uses only part of the kinetic energy of the flywheel. The difference is in the use of clutch to terminate the heating phase by friction before the normal braking of the rotational movement of the total inertial mass, thus avoiding torques at the end of the friction process, as is usual with the previous method.

The most widespread industrial brands in the field of production of machines for friction welding are Thompson (England) and Kuka (Germany).



Fig. 15 Friction welding machine [19]

2.13 Use of friction welding in practice [3] [6] [13]

Almost all cutting tools, where their machining part is made of high-speed steel, are made of two types of materials. The cutting part of the tool is made of high-speed steel and the clamping part is made of structural steel. Rotary friction welding technology has been used to produce tools of circular cross-section, such as drills, milling cutters, drills, and reamers.

In the automotive industry, rotary friction welding is used for welding semi-finished products of drive shafts and various similar gears, or parts with a stepped longitudinal profile. Significant savings are achieved when parts are not turned from solid material, but are friction welded from pieces of circular material, or even finished.

Rotary friction welding has been also used in the production of various types of shafts, gears on the shaft, pistons and suction valves or pneumatic cylinders, see Figures 16 and 17.

Another field where rotary friction welding is used is the manufacture of pipes and sleeves, for example for the mining industry, where pipes are highly stressed by bending and pressure. Threaded shoulders are welded to these pipes by friction welding. Furthermore, components can be produced in the form of containers, where the lids of the containers are frictionally welded to the cylindrical part. Friction welding can be used in production of energy properties as it can be seen on Fig 18.

Rotary friction welding has found a wide range of uses in the production of semi-finished products for further processing, for example by machining, where it is able to create semi-finished products from two or more types of materials, which are further machined. Furthermore, it is possible to form semi-finished or finished parts by friction welding, or it has been used to repair worn surfaces of parts.

Another way to use rotary friction welding is to weld non-metallic materials, such as plastic, glass or ceramics, which are gaining more and more use in today's modern industry. For plastics, only thermoplastics are suitable, such as PVC or PE.



Fig. 16 Pneumatic cylinder [34]



Fig. 17 Shaft [34]



Fig. 18 Exhaust turbine [34]

2.14 Advantages and disadvantages of friction welding [4] [10] [11] [13]

The friction welding method has following advantages:

- heating of welded materials takes place in a narrow zone
- no alloys are burned
- basic materials do not melt; no cracks are formed when the temperature is high
- after welding, the grain becomes finer
- due to the thermomechanical method of processing in the welding process, it yields a joint with very good mechanical properties
- compared to other welding methods, this process consumes less energy
- ecology, cleanliness and hygiene of work, no fumes are formed as with arc methods
- welding takes place in the absence of air to the contact surfaces, there is no oxidation
- the process can be easily automated
- low welding temperature
- high labour effectivity and short production times
- there are no large deformations of the welded parts as in arc welding
- no additional material and protective atmosphere required
- applicable for a wide range of various materials which can't be welded conventionally

The disadvantages may include, for example:

- welding equipment is usually more expensive
- the quality of the joint may be affected by the amount and distribution of non-metallic inclusions (stainless steel, free-cutting steel)
- possibility of formation of undesired low-melting and intermetallic phases
- the possibility of a decrease in hardness around the weld during hardened or hardened welding materials.

Rotary friction welding is mostly used for welding rotating components such as shafts, gears and components for the transport industry. See Fig. 19 and 20



Fig. 19 Friction welded shaft [20]



Fig. 20 Friction welded gear [20]

3 TESTS OF ROTATION FRICTION WELDS

3.1 Destructive testing of welds

3.1.1 Tensile test [3] [21]

The tensile test is a basic static mechanical test. The output of this test is a dependence of the stress on deformation of a tested body. The test specimens are machined in basic and well-defined shapes, usually of circular or rectangular cross-sections, which are attached to the jaws of the testing machine. A strain gauge is then attached to the sample. It records the dependence of the applied force F on the elongation of the test specimen ΔL . From this data output a tensile diagram with the values of ultimate strength and slip, elongation, contraction is compiled. Two kinds of tensile tests are distinguished. The difference is in the orientation of the test bar against the axis of the welded joint. In the transverse tensile test, the test specimens are placed transversely to the welded joint, see Fig. 21.

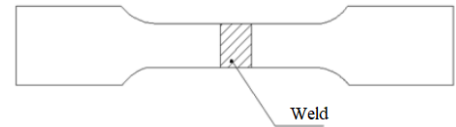


Fig. 21 test specimens for tensile test [35]

3.1.2 Charpy impact test [3] [21]

The bending impact test belongs to the group of dynamic tests, where it determines the impact work K , or the work that is needed to break the test specimen. The principle is based on breaking a test specimen with a Charpy hammer in one go. The test specimen is provided with a V-shaped or U-shaped notch with standard defined dimensions in the diagonal direction with respect to the weld as it is shown in Fig 22.

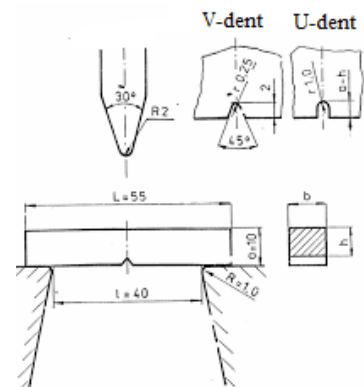


Fig. 22 test specimen for Charpy impact test [36]

3.1.3 Bending test [3] [21]

The bending test is a static test. As in the tensile test, the test bar is placed longitudinally or transversely to the weld axis. During the test, plastic deformation occurs by unidirectional bending, which causes tensile and compressive stresses. The loading of the specimen is caused by a slow gradual loading in the weld axis. It distinguishes two types of loading. On the bending mandrel (Fig. 23) and bending pulley.

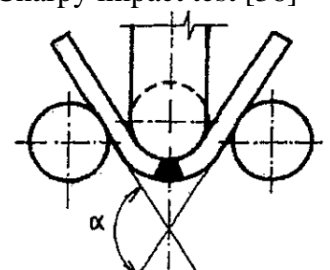


Fig. 23 bending test [37]

3.1.4 Hardness test [3] [21]

The purpose of the hardness test is to determine the lowest and highest hardness values of the base material, the material in HAZ and the weld metal. Hardness is defined as the resistance of a material to the ingress of a foreign body. Vickers or Brinell hardness measurements are most often used.

A problem in testing hardness (microhardness) can be the thermal influence of the sample during mechanical cutting, which is performed perpendicular to the welded joint. Hardness tests are indicated by the letter R (for several impressions) or the letter E. (Fig 24)

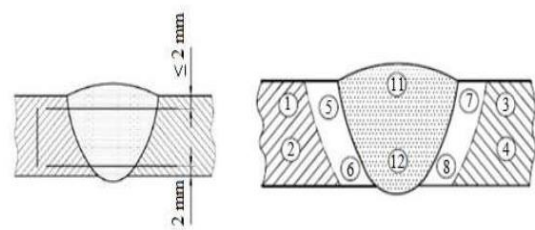


Fig. 24 Position of hardness test in welds [38]

3.2 Metallographic tests of welds

Metallographic tests are a frequently used supplement to tests of mechanical properties in the verification of welded joints. According to the magnification used, metallographic tests are divided into macroscopic and microscopic. The tests can be performed in an unetched or etched state and find their application in the detection of macroscopic or microscopic characteristics of the welded joint.

3.2.1 Macrostructure

Macrostructure evaluation often precedes microstructure evaluation and is often crucial in confirming or refuting quality. The macroscopic test is performed by eye examination or at low optical magnification (up to a maximum of 3 times magnification). The inspection is performed on a test specimen taken transversely to the weld axis, which includes the weld metal, the heat affected zone and the base material. For welded joints, it belongs to the basic test of weld quality. After grinding, polishing and possible etching of the sample surface, it allows to assess the following properties:

- presence of defects
- shape of weld
- layers of weld
- connection of weld layers
- shape and range of HAZ

A Carl Zeiss Stemi 508 stereomicroscope was used for this test, which is shown in the fig 25.

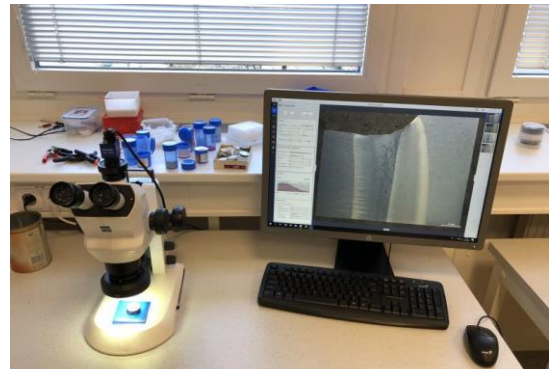


Fig. 25 Carl Zeiss Stemi 508

3.2.2 Microstructure

Microstructural analysis is performed using a microscope with multiple magnifications. Light microscopes (magnification up to 1000x) or confocal laser microscopes (magnification up to 10,000x) are used for this method. As with the macroscopic test, the inspection is performed on test specimens oriented transversely to the axis of the welded joint.

The preparation of samples for microscopic examination is much more laborious than macroscopic testing, as any errors in preparation may result in incorrect evaluation. The sample preparation methods must be chosen so that the controlled surface is not affected. Etching is usually used for better sample surface quality. Etching is performed by immersion in an etchant, or by electrolytic etching.

Microscopic inspection can be compared:

- individual grains of material
- grain boundaries
- structural components of weld and HAZ

Olympus GX51 light microscope and camera Nikon DS-Fi 1 were used to capture pictures as seen in Fig 26.

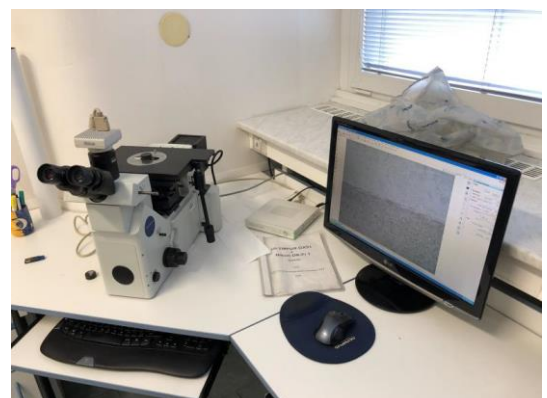


Fig. 26 Olympus GX51 with camera Nikon DS-Fi

3.3 Tensile tests of friction welded joints

Another part of the experimental section is the tensile test, which is performed by uniaxial loading in the axis of the welded sample. The tensile test is performed at room temperature in the range of $10^{\circ} \div 35^{\circ} \text{C}$, if necessary, the temperature can be increased or decreased by external heating or cooling, depending on the operating conditions of the welded joint. The aim of the test was to determine how much load the sample will break at the weld between the individual materials. Two samples of basic materials were used for the test, namely AISI 316L and Ti GR2 to verify the ultimate strength of the material and to calibrate the machine for tensile testing.

The method of clamping is a very important part of the tensile test, as it wanted to be manage a uniaxial load in the axis of the tested specimen. The test rod can also be preloaded to achieve ideal alignment. In our case, the samples had a length in the range of 160-170 mm. As it can be seen in the figure 27, this length guaranteed a sufficiently strong clamping in the tearing machine. The test rod does not correspond to the dimensions according to the ČSN EN 10002-1 standard; therefore, this test is not standardized. The samples were not equipped with a shoulder for clamping, special clamping jaws were used, which guaranteed sufficient clamping for the experiment.



Fig. 27 Tensile test rod

Universal machines are used to perform the tensile test, which can perform tensile, compressive or bending tests. The machines can load the test specimen statically or dynamically and are equipped with various sensors of rod elongation and required forces. The drive is either mechanical or hydraulic. The hydraulic drive is used for loads greater than 200 kN. In this case, a hydraulic testing machine ZD40 was used, which is employed at the university. The parameters is shown in attachment 1. The scheme of the testing machine is shown in the fig 28.

The test speed is the speed of movement of the movable cross member of the machine and is given by the modulus of elasticity of the material. Voltage rate is defined as the increase in voltage per unit time. The value of the load speed is in the range of $2 \div 20 \text{ MPa} / \text{s}$. In our case, a loading speed of $10 \text{ MPa} / \text{s}$ was used.

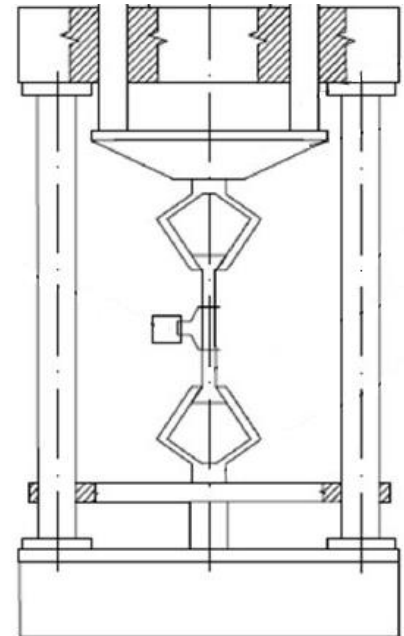


Fig. 28 Scheme of hydraulic testing machine [39]

3.4 Sample preparation

Welded specimens must be properly prepared for proper evaluation of macrostructure and microstructure. Four samples of welded joints were supplied for grinding. Homogeneous welded joints made of stainless steel AISI 316L and titanium TI GR2 and two heterogeneous welded joints made of the mentioned materials, one of which was modified by removing the protrusion by turning. The first step is to select a place for taking a future sample, which should be representative and characterize the technology used, at the same time it should be affected as little as possible by heat and deformation. The welded samples were delivered by the company in a shortened state, for better handling and subsequent processing of the samples.

The second step was to cut the samples. The cut was made perpendicularly to the welded joint, along the axis of the welded specimen, with metallographic saw Secotom 60 (Fig.29), with cutting disc Struers (Fig. 30) is suitable for cutting hard materials. There was a problem with the division of the samples, as it is not common to divide welded joints from such different materials, therefore the parameters of the rotation speed were adjusted to 2200 rpm and a slower feed was chosen. To eliminate the thermal influence of the sample as much as possible, the process was liquid cooled. Distilled water with Corrozip additive solution was selected as the liquid to prevent corrosion of the metallographic saw.

The next phase of preparation was followed by preparation and attachment of the samples. After cutting on a metallographic saw, the samples were rinsed with water and alcohol and placed on a separator-coated heated cylinder of a Struers Citopress 15 (fig. 31) pressure press and backfilled with a suitable amount of Multifast resin. Subsequently, the press was closed, and a 5-minute program was started, in which it was heated to 180 °C at a pressure of 250 bar for 3 minutes and then cooled for 2 minutes. The resulting pellet dimensions were 30 mm in diameter and 12 mm high. After removal from the press, the edges of all samples were chamfered for better handling and to avoid damaging the sandpaper and polishing cloths.

All samples were first ground to minimize surface irregularities. A Tegramin 20 metallographic grinder from the Struers brand (Figure 32) was used for this. The samples were clamped in the carrier and ground as needed at several minute intervals (in chart 2) with a constant supply of distilled water. Abrasive papers were changed with decreasing grain size from coarser to finer. After each grinding, the samples were cleaned of abrasive. Sanding papers made of silicon carbide with individual grit sizes (in the figure 33) were used, grinding times for individual grit sizes are assigned in the table.



Fig. 29 Struers Secotom 60



Fig. 30 Struers cutting disc



Fig. 31 Struers Citopress 15

Chart 2 intervals of grinding for abrasive grain

| grit size | μm | Grinding time |
|-----------|-----|---------------|
| SiC 220 | ~90 | 5 min |
| SiC 600 | ~30 | 2÷3 min |
| SiC 1200 | ~15 | 2÷3 min |
| SiC 2400 | ~10 | 2 min |
| SiC 4000 | ~5 | 1 min |



Fig. 32 Struers Tegramin 20

Grinding was followed by polishing on the same equipment, only instead of sandpaper polishing cloths were used and instead of water polishing paste containing diamond particles with grain sizes of 9 μm, 3 μm and finally 1 μm was dosed. The lubricant isopropyl alcohol was used for better polishing. The polishing time was again in several minute intervals, as needed. As with grinding, the samples needed to be thoroughly rinsed with water, then alcohol and dried with a hot air gun between changes in the polishing paste. The polishing process was complete when no sanding scratches were visible on the surface. The load used for grinding and polishing the specimens was first 35 N and then reduced as needed. For diamond pastes, a load of only 5 ÷ 10 N is used. The rotation of the disc is consecutive and the speed of rotation of the disc is in the range of 100 ÷ 200 rpm, for the clamping head the rotation speed is 150 rpm. To highlight the structure, all samples were subsequently etched. Kroll and Marble solutions were used for etching (see charts 3 and 4). The solution etching time was chosen for 28 seconds for Titanium Ti GR 2 and 2 seconds for AISI 316L stainless steel.



Fig. 33 Sanding papers

Chart 3 Kroll solution

| | H ₂ O [ml] | HF [ml] | HNO ₃ [ml] |
|-------|-----------------------|---------|-----------------------|
| Kroll | 50 | 1,5 | 3 |

Chart 4 Marble solution

| | H ₂ O [ml] | H ₂ SO ₄ [ml] | HCl [ml] | CuSO ₄ [g] |
|--------|-----------------------|-------------------------------------|----------|-----------------------|
| Marble | 100 | 50 | 100 | 20 |

3.5 Non-destructive weld testing

3.5.1 Visual test [3] [5] [10]

It has been visually verified defects only on the surface. It is the simplest, most affordable, and cheapest method of weld inspection. The inspection of the weld takes place with the naked eye or with optical devices with multiple magnifications (magnifier). The testing should be performed under good lightning conditions. The test is divided into a direct method, where it looks for defects directly with the eye, or an indirect method, where it has been used, for example, an endoscope. Good cleaning of the welded joint is important in this test. It usually takes place as the first test.

3.5.2 Penetrative test [3] [5] [10]

By capillary test defects has been detected only on the surface. It uses capillary phenomena, especially wettability and capillarity. The test itself is preceded by several steps. The first is perfect surface preparation by degreasing, then applying a test liquid (such as kerosene) to the test surface and removing excess test liquid. The second step is to apply a developer (for example zinc oxide in acetone). The last step is the surface inspection and evaluation. It can be seen in Figure 34.

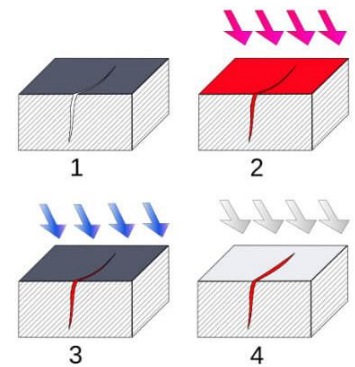


Fig. 34 Penetrative test [40]

3.5.3 Magnetic powder test [3] [5] [10]

The principle is based on the visibility of magnetic field lines projecting on the surface of the material and potential defects. This method detects surface or shallow subsurface defects. The disadvantage is that this method is only for ferromagnetic materials. UV light is used to make the defects more visible, as shown in Figure 35.

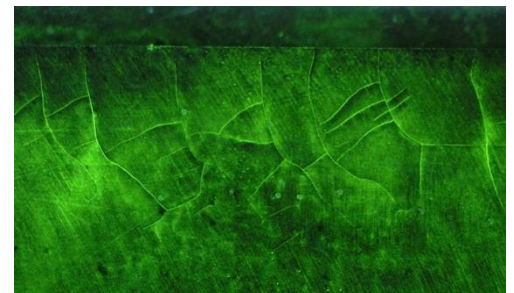


Fig. 35 Magnetic powder test [41]

3.5.4 Ultrasonic test [3] [5] [10]

This test uses the propagation of ultrasonic waves through the material, their reaction to changes in the material and their subsequent detection. Two methods of ultrasonic testing have been distinguished. In the pass-through method, defects create a reduction in sound pressure, which is noted in the difference between the transmission value and the reception value.

With the reflective method (Fig. 36), short ultrasonic pulse has been sent to the material and the defects delay it depending on the size of the defect. This test is used to indicate subsurface defects throughout the thickness of the material.



Fig. 36 Ultrasonic test [42]

3.5.5 Radiation test [3] [5] [10]

The principle is based on the detection of internal defects using electromagnetic radiation or gamma radiation. Individual defects partially absorb the radiation, and this is then reflected on the detector. Defects are shown on it as darker areas.

4 WELDED MATERIALS

The selected welded materials are AISI316L and TI GR2 steel.

4.1 Steel AISI 316L [22] [23] [24]

Alloy 316L is a chromium-nickel-molybdenum austenitic stainless steel developed to provide improved corrosion resistance in moderately corrosive environments. Chemical composition is shown in chart 5. It is often utilised in process streams containing chlorides or halides. The addition of molybdenum improves general corrosion and chloride pitting resistance. It also provides higher creep, stress-to-rupture, and tensile strength at elevated temperatures. The alloy resists atmospheric corrosion, as well as, moderately oxidizing and reducing environment. It also resists corrosion in polluted marine atmospheres. The alloy has excellent resistance to intergranular corrosion in the as-welded condition. The alloy has excellent strength and toughness at cryogenic temperatures. The thermal conductivity of titanium is $21,9 \text{ W}\cdot\text{m}^{-1}\cdot\text{K}^{-1}$. The specific heat capacity of titanium is $523 \text{ Jkg}^{-1}\cdot\text{K}^{-1}$. Alloy 316L is non-magnetic in the annealed condition but can become slightly magnetic as a result of cold working or welding. It can be easily welded and processed by standard shop fabrication processes. Certificate of material AISI 316L is shown in attachment 2.

Chart 5 chemical composition of AISI 316L [25]

| Element tag | C | Cr | Si | Mn | Mo | Ni | N | P | S |
|-------------|--------|-----------|-------|------|---------|-----------|-------|--------|--------|
| Content % | ≤0,035 | 16,0-18,0 | ≤0,75 | ≤2,0 | 2,0-3,0 | 10,0-15,0 | ≤0,11 | ≤0,040 | ≤0,030 |

4.2 Titanium Ti GR 2 [26] [27] [25]

Ti Grade 2 is a commercially pure titanium grade with excellent biocompatibility and good mechanical properties. The achievable yield strength compares to that of austenitic stainless steels. Interstitially dissolved elements in small quantities increase the corrosion resistance. Titanium Grade 2 is widely used in many different applications that require strength, ductility, and low density, potentially surrounded by corrosive media. Ti Grade 2 can be used in continuous operation at temperatures up to 425 °C, operation at up to 540 °C is possible for a short time. The thermal conductivity of stainless steel is $15.5 \text{ W}\cdot\text{m}^{-1}\cdot\text{K}^{-1}$. The specific heat capacity of stainless steel is $468 \text{ Jkg}^{-1}\cdot\text{K}^{-1}$. Typical applications in medical engineering or heat exchangers in energetics. Further possible applications can also be found in aircraft and electrochemistry. Chemical composition is shown in chart 6. Certificate of material Ti GR2 is shown in attachment 3.

Chart 6 Chemical composition of TI GR2 [26]

| Element tag | C | O | Fe | N | H |
|-------------|-------|-------|-------|-------|--------|
| Content % | ≤0,08 | ≤0,25 | ≤0,25 | ≤0,03 | ≤0,015 |

5 DESIGN AND EXECUTION OF THE EXPERIMENT

The aim of the experiment is to determine the weldability of stainless steel AISI 316L and titanium Ti GR 2 by means of rotary friction welding for future introduction into serial production. Welding of these materials by conventional methods has many problems that could be eliminated by friction welding. Friction welding took place on a semi-automatic lathe to determine the weldability on this universal device. The aim was to create a full-fledged welded joint that could be used in technical practice.

To evaluate the quality of the welded joint created by rotary friction welding, a metallographic test of the macrostructure was used to evaluate the shape of the welded joint. Furthermore, such a test was used at the request of the company's representatives to determine the values of the welded joint, whether the values are satisfactory or not. None of the tests took place according to the standard but based on consultations with the supervisor.

5.1 Production of semi-finished products for rotary friction welding

To perform an experiment to determine the weldability of stainless steel AISI 316L and titanium Ti GR2, round bars with a diameter of 10 mm were selected. A total of 16 samples of heterogeneous welds were prepared. 8 welds were prepared for welding without preheating and another 8 for welding with preheating. Welding blanks were made in a uniform length of 85 mm to measure the shortening of materials during welding. Turning technology was used to save time and then weld the pieces on the same machine.

As already mentioned, a semi-automatic lathe with stepless speed control and a handbrake was used for rotary friction welding. These requirements are very important for the creation of quality friction welds. Handbrake has been required to stop rotation. Forging pressure cannot be used, when the welded parts rotate, this leads to a significant reduction in joint strength. Jigs were used for clamping (in the picture 37 and 38) The pressure required for welding was derived from the sliding poppet. Heating in friction welding with preheating was realized by an oxy-acetylene flame.



Fig. 37 Rotation Jigs



Fig. 38 Static jigs

5.2 Welding process

The individual parameters of the friction welding process were constant, except for the rotational speed, which it has been chose in the range of 500 to 800 rpm. The specific friction pressure was derived by a poppet feed of 5 mm in 1 sec and the forging pressure was chosen to be 10 mm in 1 sec. The friction time for individual friction processes can be seen in chart 7.

Chart 7 Friction welding parameters

| | Friction speed [rpm] | Friction time [s] | Forging time [s] |
|--|----------------------|-------------------|------------------|
| Homogenous weld AISI 316L | 1000 | 8-10 | 2-4 |
| Homogenous weld Ti GR2 | 800 | 4-5 | 2-4 |
| Heterogenous weld AISI 316 and Ti GR2 | 800 | 4-5 | 2-4 |

5.2.1 Welding process of AISI 316L and Ti GR2

The welding process itself proceeded according to the known steps of rotary friction welding, which were as follows. The first step was the correct clamping of the welded materials into the jig on the machine. Better results have been obtained by clamping stainless steel to the machine chuck, as shown in Figure 39, and titanium to a sliding poppet fixture. The unloading of the welded materials from the clamping jigs was 10 mm, because with a larger unloading there was a decrease in the rigidity of the clamping and undesired vibrations, which resulted in the formation of a poor-quality welded joint.

The second step was to turn on the machine and contact the welded materials. The third step is to derive the specific friction pressure for a specific friction time. In Figure 40 the contact surfaces are heating up, which was visible after 3 seconds of welding. After approximately 5 seconds of welding, a Ti GR 2 reaction occurred, which began to spark when the welding temperature was reached, as shown in Figure 41.



Fig. 39 clamping of welded materials



Fig. 40 Contact of welded materials

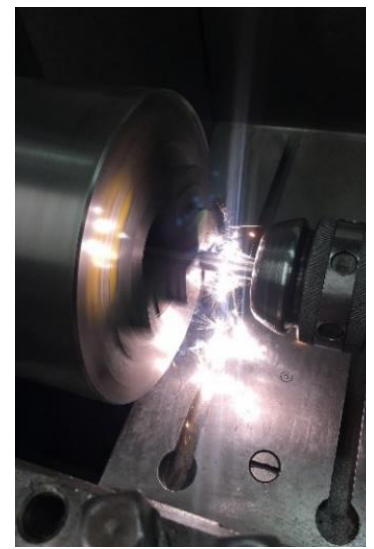


Fig. 41 sparks in friction process

The fourth step is to create a sufficient burr of materials to form a suitable weld, as shown in Figure 42. The fifth step follows, and that is to stop the speed after a sufficient burr of material has formed.

After stopping the speed, the sixth step follows, which is the derivation of the specific forging pressure for the duration of the forging time. This step is very important, because the derivation of the specific forging pressure creates the desired properties of the welded joint. It was applied for approximately 3 seconds. The whole process is shown in Figure 43

The last step is the relaxation of the welded joint. Welded materials are removed from the jigs and are set aside for cooling and other processing options, such as turning the resulting burr.



Fig. 42 forming suitable weld



Fig. 43 application of forging pressure

The resulting welded joint does not have the classic shape of the burr, this is due to the different physical properties of the welded materials. AISI 316L stainless steel is characterized by a higher heat capacity and lower thermal conductivity compared to titanium Ti GR 2, so during the welding process it has been seen that only titanium Ti GR 2 was melted and flowed around stainless steel AISI 316L. The resulting weld created by rotary friction welding can be seen in Figure 44. The picture shows that the beginning of the burr is slightly frayed, this is due to unevenness on the surface, oxides on the surface of the material and their exclusion into the protrusion.

In friction welding, the shortening of materials must be considered, as a burr is formed to create a welded joint. In our case, only titanium Ti GR 2 was melted. To create a burr measuring approximately 10 mm, the addition of titanium of a similar length is required.



Fig. 44 Final weld

5.2.2 Welding process of AISI 316L

The procedure for welding AISI 316L stainless steel is identical to the one in previous chapter, with rotations adjusted to 1000 rpm. This seemed to be optimal due to sufficient heating of the contact surfaces of the material. The friction time to form a sufficient burr was twice as long, as it took a longer time to heat the contact surfaces. The unloading of the material from the fixture was 7 mm, to eliminate vibrations that were greater due to the greater strength of AISI 316L stainless steel. During the welding of stainless steel, both parts of the materials melted, and a symmetrical outgrowth of both materials was formed.

As it can be seen in the figure 45, the burr is very rough, this was due to the mechanical and physical properties of the material and the construction of the fixtures, as there was a slight vibration of the materials during welding.



Fig. 45 AISI 316L final weld

5.2.3 Welding process of Ti GR 2

The procedure for welding titanium Ti GR 2 is identical to the one in previous case. Rotations of 800 rpm were used, since at this speed the weld exhibited best burr formation. The friction time was approximately one third compared to AISI 316L stainless steel, as the specific heat capacity and thermal conductivity resulted in rapid heating and heat transfer through the material. The lining, like the welding of heterogeneous welds, was 10 mm, as titanium is softer than stainless steel and the formation of a weld does not generate too much vibrations as the previous method mentioned in chapter 5.2.2. During the welding of titanium, a symmetrical burr was formed in the same way as in stainless steel, which was accompanied by a sparking reaction when the welding temperature of titanium Ti GR 2 was reached. In this case it was due to surface inequalities and the reaction of titanium to temperature and start sparking. The burr is very rough as can be seen in figure 46.

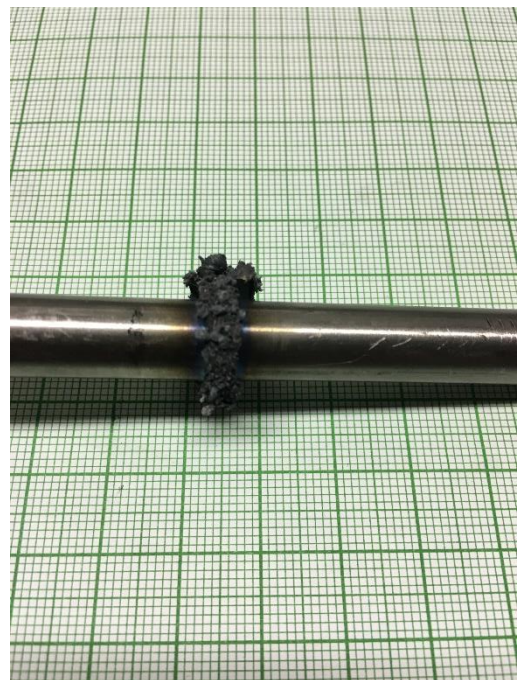


Fig. 46 TI GR2 final weld

5.3 Evaluation of macrostructure

In the case of homogeneous friction welds, they were subjected to a macrostructure test after etching, which was observed and then photographed. It is visible that penetration occurred across the entire contact plane. Figures 46 and 47 include summary of the macrostructure of both samples of homogeneous welded joints at 0.34 times magnification.

The figure 47 of sample 1 shows a homogeneous welded joint of AISI 316L stainless steel. On the left and right side, it can be seen the basic material, in the central area it can be seen the weld itself. A symmetrical outgrowth is clearly visible. Further, in the direction from the weld to the base material, in both directions there is a thermo-mechanically affected area and a thermally affected area, their widths being measured from the centre of the weld. On the sample, the largest width of the thermo-mechanically affected area is about 3 mm and the thermally affected area is about 4 mm. The areas

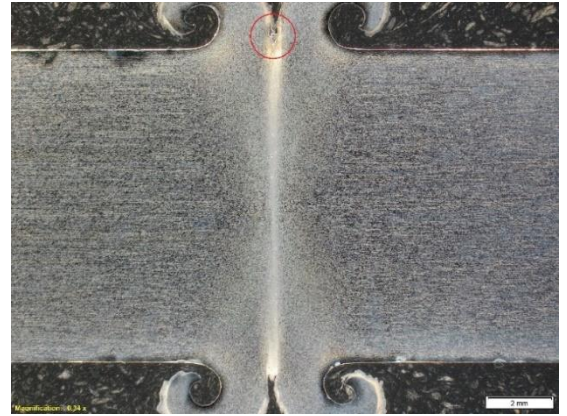


Fig. 47 Macrostructure of AISI 316L

on the outer edge of the welded sample reach the highest values and decrease towards the centre of the sample. This shape of the affected areas is determined by the forging phase. After stopping, the welded parts are pressed together by a specific forging pressure, because of which the plasticized material is extruded from the centre to the edges of the welded material. In sample 1, a crack marked in red in Figure 49, can be seen in the centre of the welded joint.

The figure 48 of sample 2, as with sample 1 shows the base material is on the left and right and the weld is visible in the middle. It has a different shape compared to sample 1. As in the previous case, two areas are visible. The first thermo-mechanically affected reaches the highest values of 3 mm at the outer edge of the sample. The second heat-affected zone reaches higher values than stainless steel due to greater thermal conductivity and lower heat capacity. Its values reach the highest values of 5 mm at the outer edge of the sample. Towards the centre both values decrease. This is caused by forging phase in friction welding as in sample 1. Compared to the welded joint of AISI 316L stainless steel, there are no cracks in the welded joint of titanium Ti GR2 and the welded joint is solid. In the Ti GR2 weld, the area of the extruded plasticized material is more pronounced.



Fig. 48 Macrostructure of Ti GR2

In the case of heterogeneous welded joints, it could be seen after grinding that there was no penetration across the entire weld area. This is due to the different thermal capacity and thermal conductivity. The Ti GR2 material was heated to the welding temperature, but the AISI 316L material was not sufficiently heated. The Ti GR2 was therefore wrapped around the AISI 316L. The resulting burr is only one-sided, formed by melting only Ti GR2.

5.4 Evaluation of microstructure

From the observations of the microstructure of homogeneous welds of AISI 316L stainless steel (Fig 48) it was concluded that the material has an austenitic structure. The structure is difficult to be seen because the pits were etched into the sample. This was caused by a bad etching time, or a slight change in the etchant. However, welding has taken place over the entire weld area. The etching highlighted the transition part of the weld. The transition part is in many dimples.

Another sample examined was titanium Ti GR2 (Fig49). At first glance, the examined areas were scratched during sample preparation. This could be solved by adjusting the grinding parameters during sample preparation. The welded joint is formed over the entire surface of the welded surfaces. There are no obvious errors in the welded joint. In the transition area, the structure created by the welding process is refined. The two welded samples were perfectly mixed. The last examined sample is a heterogeneous weld made of AISI 316L and Ti GR2 materials (Fig 50 and 51). Plastic deformation of both welded materials can be seen on the contact surfaces. The materials were not mixed. The mechanical connection was made by wrapping titanium around the stainless steel and on the contact surfaces. Since the contact surface of the stainless steel was not melted, an oxidized layer formed on the contact surface of the titanium. It was created by heat at the weld but was not pushed into the burr.



Fig. 49 Microstructure of AISI 316L weld
(10x zoom)



Fig. 50 Microstructure of Ti GR2 weld
(10x zoom)



Fig. 51 Microstructure of AISI 316L and Ti
GR2 weld (20x zoom)



Fig. 52 Microstructure of AISI 316L and Ti
GR2 weld (150x zoom)

5.5 Execution and evaluation of tensile test

One of the main requirements of Tecpa s.r.o for possible industrial application was heterogeneous welded joint testing by uniaxial tensile loading. The aim was to determine the yield strength, tensile strength and maximum load force, and which method of production of the welded joint is better. For the tensile test, 16 samples were broken for rupture, 8 welded without preheating and 8 welded with preheating. Each sample was loaded into the testing machine and subsequently loaded with tensile loading speed value of 10 MPa/s.

To verify the mechanical properties and to calibrate the testing machine, welded AISI 316 and Ti GR2 materials were broken. For samples without initial preheating an average strength limit of 235.44 MPa was reached. The average value of the maximum loading force was 18,491.45 N. As the welded joint did not show plastic deformation during the tensile test, the yield strength is not included in the results.

For samples that were preheated an average tensile strength of 174.15 MPa was reached. The average value of the maximum loading force was 13,665.05 N. As with the samples made without preheating, the welded joint did not exhibit plastic deformation. Therefore, the yield strength values are not included in the results of the tensile test.

Upon closer inspection of the point of rupture (Figure 52 and 53), it is evident that the fracture occurred at the contact plane of the welded surfaces. The materials were not mixed during friction welding, but only the stainless steel AISI 316L was bypassed with titanium Ti GR2 and the welded parts were mechanically joined. The tables show the individual measured values during the tensile test (charts 7 and 8). Values are shown in bar graph for easier visualisation (graph 1-4). The parameters of hydraulic testing machine is shown in attachment 1.



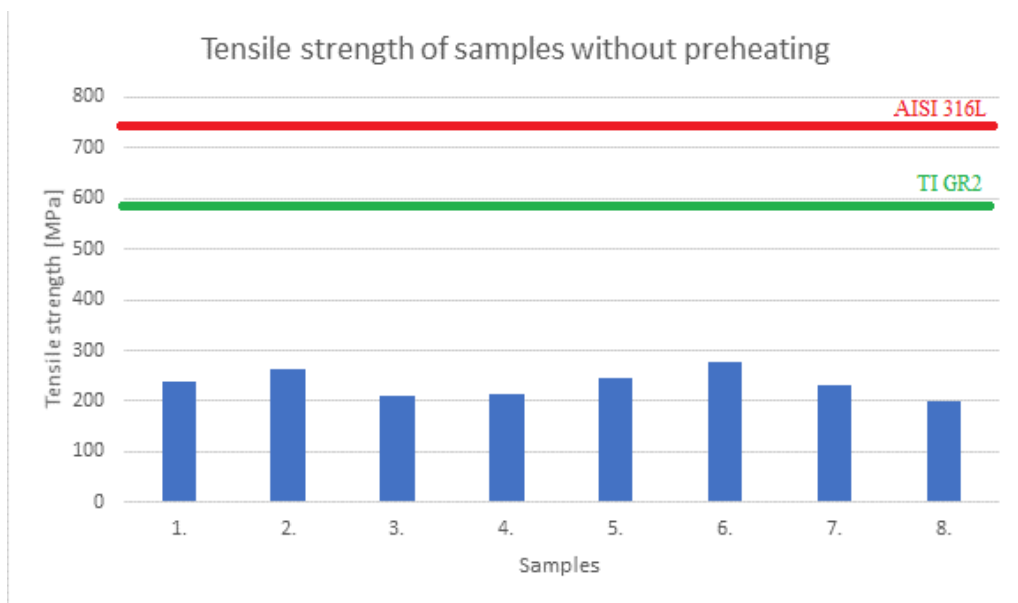
Fig. 56 Cracked friction weld after tensile test



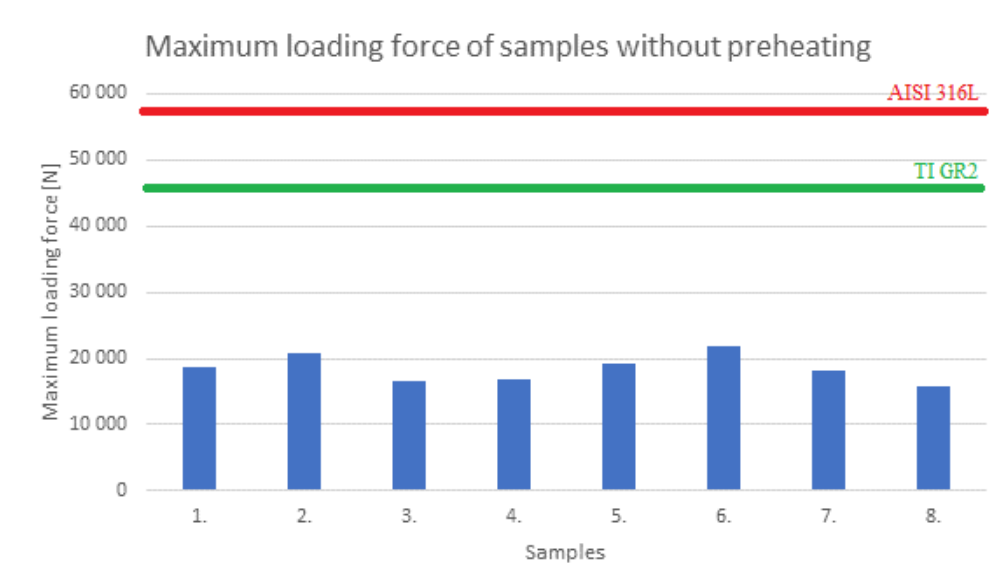
Fig. 57 Detail of friction weld after test

Chart 8 values for samples without preheating

| Samples without preheating | F_m [N] | R_m [MPa] |
|----------------------------|-----------|-------------|
| 1 | 18 762,0 | 238,8846 |
| 2 | 20 718,0 | 263,7891 |
| 3 | 16 617,6 | 211,5814 |
| 4 | 16 824,4 | 214,2144 |
| 5 | 19 175,6 | 244,1507 |
| 6 | 21 893,6 | 278,7573 |
| 7 | 18 150,4 | 231,0975 |
| 8 | 15 790,0 | 201,0441 |



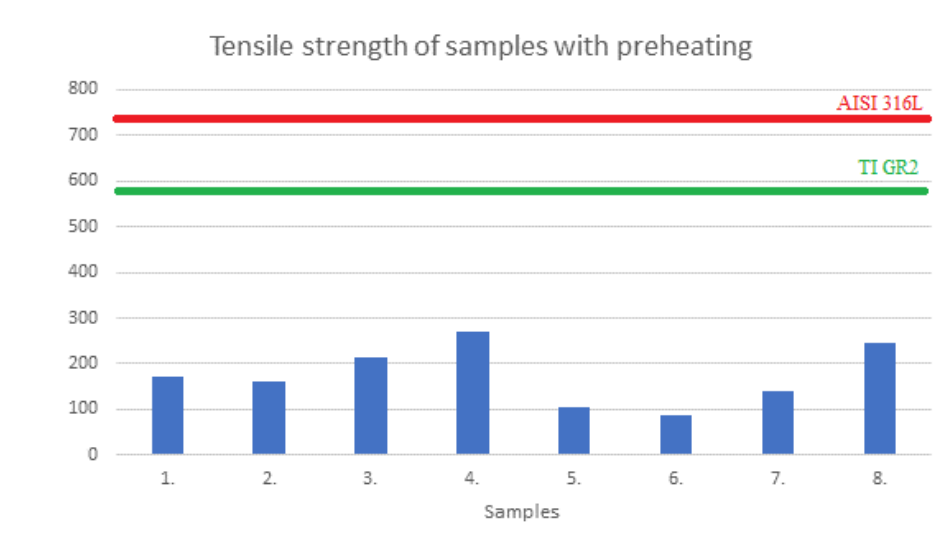
Graph 1 Tensile strength of samples without preheating



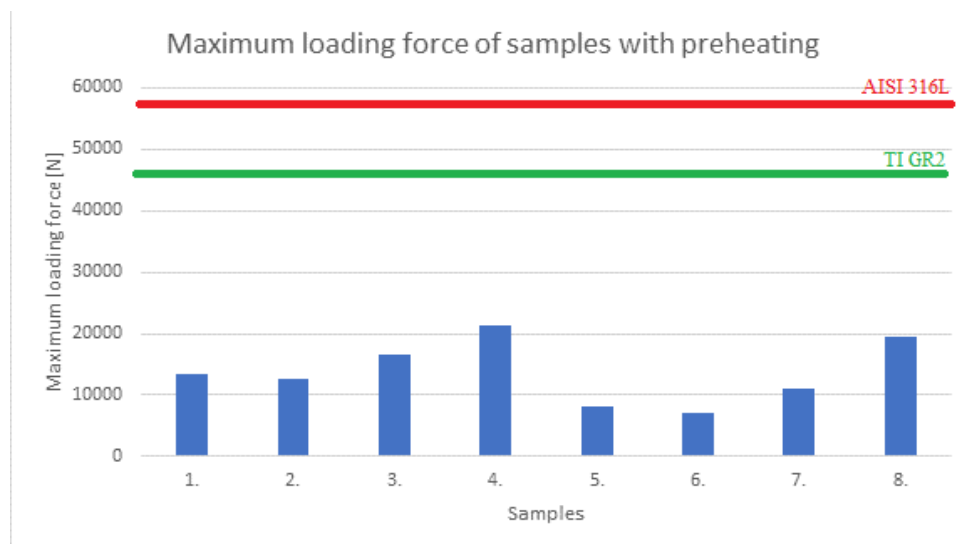
Graph 2 Maximum loading force of samples without preheating

Chart 9 values for samples with preheating

| Samples with preheating | F_m [N] | Rm [MPa] |
|-------------------------|-----------|----------|
| 1 | 13 412,0 | 170,7665 |
| 2 | 12 640,4 | 160,9422 |
| 3 | 16 684,8 | 212,4370 |
| 4 | 21 227,6 | 270,2776 |
| 5 | 8173,2 | 104,0642 |
| 6 | 6978,8 | 88,85663 |
| 7 | 10 957,2 | 139,5111 |
| 8 | 19 346,4 | 246,3254 |



Graph 3 Tensile strength of samples with preheating



Graph 4 Maximum loading force of samples without preheating

6 CONCLUSIONS

The aim of this bachelor's thesis was to conduct a literature research on the topic of rotary friction welding. An experimental part was subsequently developed, in which AISI 316L and Ti GR 2 materials were welded together. These joints were subsequently tested by tensile test. The final part was the examination of the macrostructure and microstructure under a microscope.

The first part of the bachelor thesis explained the basic theoretical concepts related to friction welding of materials. These theoretical starting points were used to develop the experimental part of the bachelor's thesis.

The experimental part of the bachelor thesis was focused on the creation of welded joints of heterogeneous materials AISI 316L and Ti GR2 using rotary friction welding and their subsequent testing – whether they meet the requirements for use in industry. Welds of individual materials were also formed to test the feasibility of the experiment.

After inspecting the samples after grinding and images from the macrostructure, it was obvious that the heterogeneous materials did not penetrate the contact surfaces. Only the Ti GR 2 was wrapped around the AISI 316L and a mechanical connection was formed rather than a mixing connection. Even the subsequent application of preheating did not affect the mixing of materials.

After inspecting the images of the macrostructure of homogeneous welded joints from individual materials, it was obvious that the individual parts were mixed. For the AISI 316L material, a symmetrical burr was formed. The heat affected area was symmetrical and reached values of 4 mm. Cracks formed in the transition between the individual surfaces on the outside of the weld sample. Cracks initiate stress and the formation of other defects that could result in tearing of the welded joint. For the Ti GR2 material, a weld was formed with an uneven burr. A similarly large heat-affected zone was formed, reaching values of 5 mm. The welded joint did not show cracks, as in the AISI 316L material.

Subsequently, the heterogeneous welded joints were tested by a tensile test. At first glance, it was clear that there was no plastic deformation during the tensile test. The samples, which were welded without preheating, reached higher values. For samples without preheating, the maximum loading force was 18,491.5 N and the yield strength reached 235.4 MPa. For specimens that were welded with preheating, a maximum loading force of 13,677.6 N and a strength limit of 194.1 MPa were achieved. The results were compared with the results of the basic materials AISI 316L and Ti GR2, where it was found that the samples reached one third of the values.

Overall, it can be said that the results do not reach the required values for industrial use. In depth research will be carried out on modifications of parameters or methods of welding, for example modification of the welding environment, or welding with additional material. The results served as a cornerstone for research into the welding of AISI 316L and Ti GR2 materials.

BIBLIOGRAPHY

- [1] ČSN EN ISO 4063. : *Svařování a příbuzné procesy - Přehled metod a jejich číslování*. Praha: Český normalizační institut, 2001. Třídící znak 05 0011.
- [2] *Materiálové normy: Ferona* [online]. Ferona, 2017 [cit. 2021-02-04]. Dostupné z: <https://online.ferona.cz/materialove-normy/>
- [3] PLÍVA, Ladislav a Jiří KAHOUN. *Svařování třením v praxi*. 1. vyd. Praha: Státní nakladatelství technické literatury, 1973.
- [4] AMBROŽ, O., B. KANDUS a J. KUBÍČEK. *Technologie svařování a zařízení: učební texty pro kurzy svářečských inženýrů a technologů*. 1. vyd. Ostrava: ZEROSS, 2001. Svařování. ISBN 80-85771-81-0.
- [5] KUNCIPÁL, Josef. *Teorie svařování*. 1. vyd. Praha: Nakladatelství technické literatury, 1986, 265 s. ISBN MK 1622.
- [6] WEMAN, Klas. *Welding processes handbook*. 2nd ed. Oxford: Woodhead Publishing, 2012. Woodhead Publishing in materials. ISBN 978-0-85709-510-7.
- [7] KUČERA, Jan. *Teorie svařování - část 2*. 1.vyd. Ostrava: VŠB, 1994. ISBN MK 916.
- [8] SWITZNER, N. *Friction welding for cladding applications: PROCESSING, MICROSTRUCTURE AND MECHANICAL PROPERTIES OF INERTIA FRICTION WELDS OF STAINLESS STEEL TO LOW CARBON STEEL AND EVALUATION OF WROUGHT AND WELDED AUSTENITIC STAINLESS STEELS FOR CLADDING APPLICATIONS IN ACID- CHLORIDE SERVICE* [online]. 2017 [cit. 2021-02-15]. Dostupné z: <http://docplayer.net/62070462-Friction-welding-for-cladding-applications-processing-microstructure-and-mechanical-properties-of-inertia-friction-welds-of-stainless.html>
- [9] MAALEKIAN, M. *Friction welding - critical assesment of literature: Science and Technology of Welding and joining* [online]. Taylor and Francis, 2007, 738-759 s. [cit. 2021-02-06]. DOI: 10.1179/174329307X249333 ISSN 1362-1718. Dostupné z: <https://www.tandfonline.com/doi/abs/10.1179/174329307X249333>
- [10] KOVAŘÍK, R. a F. ČERNÝ. *Technologie svařování*. 2. vyd. Plzeň: Západočeská univerzita, 2000, 185 s. ISBN 80-7082-697-5.
- [11] MRŇA, L. ÚSTAV STROJÍRENSKÉ TECHNOLOGIE. *Svařování třením* [online]. [cit. 2021-02-04]. Dostupné z: http://ust.fme.vutbr.cz/svarovani/img/opory/hsv_specialni_metody_svarovani_svarovani_trenim_mrna.pdf
- [12] JEDRASIÁK, P., H.R. SHERCLIFF, A.R. MCANDREW a P.A. COLEGROVE. *Thermal modelling of linear friction welding: Materials and Design* [online]. Elsevier, 2018 [cit. 2021-02-06]. DOI 10.1016 ISSN 0264-1275. Dostupné z: <https://www.sciencedirect.com/science/article/pii/S0264127518305100>
- [13] SIGMUND, M. *Svařování elektrickým odporem a třením: Presentace do předmětu ETV*. 2019.
- [14] ADAMS, D. *Low Force, Low Upset* [online]. South Bend: Manufacturing Technology, 2019 [cit. 2021-04-26]. Dostupné z: <https://blog.mtiwelding.com/low-force-low-upset>

- [15] SIMON, J. *Low Force Friction Welding --What is it?* [online]. South Bend: Manufacturing Technology, 2017 [cit. 2021-04-26]. Dostupné z: <https://blog.mtiwelding.com/low-force-friction-welding>
- [16] KUROIWA, R., H. LIU, Y. AOKI, S. YOON, H. FUJII, G. MURAYAMA a M. YASUYAMA. *Microstructure control of medium carbon steel joints by low-temperature linear friction welding: Science and Technology of Welding and joining* [online]. Taylor and Francis, 2020 [cit. 2021-04-26]. ISBN 1362-1718. Dostupné z: <http://www.tandfonline.com/doi/abs/10.1080/13621718.2019.1600771>
- [17] *Friction weldability of materials* [online]. 2018 [cit. 2021-05-15]. Dostupné z: <https://nctfrictionwelding.com/services/friction-welding-services/>
- [18] KUKA. *Rotary friction welding* [online]. Kuka, 2020 [cit. 2021-02-04]. Dostupné z: https://www.kuka.com/-/media/kuka-downloads/imported/9cb8e311bfd744b4b0eab25ca883f6d3/kuka_brochure_friction-welding.pdf?rev=b6d636f3fc6a49efa5e8cf9aa2553920&hash=B2A0D81B8377CC67578A6A30F263F718
- [19] *Yuan-Yu Roto Friction Welding Machine* [online]. 2019 [cit. 2021-05-15]. Dostupné z: <http://nebashi.com/welding-machine.php>
- [20] *Why Friction Welding is the Future of Manufacturing* [online]. 2021 [cit. 2021-05-15]. Dostupné z: <https://spinweld.com/why-friction-welding-is-the-future-of-manufacturing/>
- [21] PTÁČEK, Luděk. *Nauka o materiálu I*. 2. opr. a rozš. vyd. Brno: Akademické nakladatelství CERM, 2003. ISBN 80-7204-283-1.
- [22] *Jakosti nerezových materiálů* [online]. inerez.cz, 2021 [cit. 2021-04-27]. Dostupné z: <https://www.inerez.cz/jakosti-nerezovych-materialu/>
- [23] *Italinox.cz: charakteristiky materiálu* [online]. [cit. 2021-02-04]. Dostupné z: <https://www.italinox.cz/plechy/charakteristika-materialu/strana-2>
- [24] *CHARAKTERISTIKA KOROZIVZDORNÝCH MATERIÁLŮ A ZÁKLADNÍ INFORMACE O POUŽITÍ, ZPRACOVÁNÍ, SVAŘOVÁNÍ A MOŽNÉ KOROZI* [online]. italinox.cz, 2020 [cit. 2021-04-27]. Dostupné z: <https://www.italinox.cz/plechy/charakteristika-materialu/strana-2>
- [25] *Datasheet: Titanium-Grade 2 (3.7035)* [online]. Metalcor GmbH, 2014 [cit. 2021-04-27]. Dostupné z: <http://www.metalcor.de/en/datenblatt/122/>
- [26] *Titanium and titanium alloys: titanium grade 2* [online]. LKALLOY, 2018 [cit. 2021-04-27]. Dostupné z: <https://lkalloy.com/cs/titanium-and-titanium-alloys/titanium-grade-2/>
- [27] *Alloys: titanium grade 2* [online]. Corrosion materials, 2020 [cit. 2021-04-27]. Dostupné z: <https://corrosionmaterials.com/alloys/titanium-grade-2/>
- [28] *Optimisation of SENT test specimen design* [online]. Norway, 2015 [cit. 2021-05-15]. Dostupné z: <https://www.twi-global.com/technical-knowledge/published-papers/optimisation-of-sent-test-specimen-design>
- [29] *Optimization by RSM on rotary friction welding of AA1100 aluminum alloy and mild steel* [online]. 2020 [cit. 2021-05-15]. Dostupné z: <https://akjournals.com/view/journals/1848/11/1/article-p34.xml>
- [30] *Welding Parameters-Metallurgical Properties Correlation of Friction Welding of Austenitic Stainless Steel and Ferritic Stainless Steel* [online]. 2012 [cit. 2021-05-15]. Dostupné z: <https://scialert.net/fulltext/?doi=jas.2012.1013.1019>

- [31] *Graphical Abstract Static Friction at Fractal Interfaces Tribology* [online]. 2016 [cit. 2021-05-15]. Dostupné z: https://www.researchgate.net/figure/Graphical-Abstract-Static-Friction-at-Fractal-Interfaces-Tribology-International-2016_fig9_283675011
- [32] *Friction Coefficient: Effects of Solid Fly Ash on Wear Behaviour of AA6063 Aluminum Alloy* [online]. 2007 [cit. 2021-05-15]. Dostupné z: <https://www.sciencedirect.com/topics/chemistry/friction-coefficient>
- [33] *Weld Zones Friction Welding* [online]. 2020 [cit. 2021-05-15]. Dostupné z: https://commons.wikimedia.org/wiki/File:Weld_Zones_Friction_Welding.jpg
- [34] *Friction Welding Products* [online]. 2001 [cit. 2021-05-15]. Dostupné z: <http://follou.com/en/product/product-45-933.html>
- [35] *Tensile test specimen* [online]. 2017 [cit. 2021-05-15]. Dostupné z: https://www.researchgate.net/figure/a-dimensions-of-tensile-test-specimen-ASTM-D-638-03-b-tensile-test-machine_fig8_319653469
- [36] *Charpy Impact Test for Metallic Materials* [online]. 2003 [cit. 2021-05-15]. Dostupné z: <https://www.totalmateria.com/page.aspx?ID=CheckArticle&site=kts&NM=94>
- [37] *Three point bending test for metalic specimens* [online]. 2018 [cit. 2021-05-15]. Dostupné z: https://scielo.conicyt.cl/scielo.php?script=sci_arttext&pid=S0718-221X2018000300333
- [38] *Hardness test for welding procedure* [online]. 2019 [cit. 2021-05-15]. Dostupné z: <https://weldinginspections.net/t/hardness-test-for-welding-procedure/585>
- [39] *Hydraulic Impact Testing Machine for Mine Anti-Impact Support Equipment* [online]. 2019 [cit. 2021-05-15]. Dostupné z: <https://www.hindawi.com/journals/sv/2019/6545980/>
- [40] *Understanding the nondestructive weld testing techniques available to fabricators* [online]. 2021 [cit. 2021-05-15]. Dostupné z: <https://weldingproductivity.com/article/put-to-the-test/>
- [41] *Magnetic Particle (MT) Inspection Services* [online]. 2021 [cit. 2021-05-15]. Dostupné z: <https://www.mistrasgroup.com/how-we-help/field-inspections/traditional-ndt/magnetic-particle/>
- [42] *Ultrasonic Testing: 10 Experts Discuss One of the Smartest Technologies in NDT* [online]. 2017 [cit. 2021-05-15]. Dostupné z: <https://www.bergeng.com/blog/ultrasonic-testing-experts-discuss-nondestructive-testing/>
- [43] *Microstructure of AISI 316L* [online]. 2017 [cit. 2021-05-15]. Dostupné z: https://www.researchgate.net/figure/Microstructure-of-1260C-60-min-vacuum-sintered-AISI-316L_fig1_322149989
- [44] *Microstructure of Grade2 titanium in the initial state.* [online]. 2012 [cit. 2021-05-15]. Dostupné z: https://www.researchgate.net/figure/Microstructure-of-Grade2-titanium-in-the-initial-state_fig1_260276153
- [45] *Investigation of weld defects in friction-stir welding and fusion welding of aluminium alloys* [online]. 2011 [cit. 2021-05-19]. Dostupné z: <https://ijmme.springeropen.com/articles/10.1186/s40712-015-0053-8/figures/3>

TABLE OF SYMBOLS AND ABBREVIATION

| designation | legend | unit |
|-------------|---------------------------------|-------|
| A_1 | Temperature | [°C] |
| A_3 | Temperature | [°C] |
| A_{Cm} | Temperature | [°C] |
| d | Diameter | [mm] |
| F | Force | [N] |
| f | Friction | [-] |
| HAA/HAZ | Heat affected area/zone | [-] |
| K | Impact work | [J] |
| n | Rotation speed | [rpm] |
| PE | Polyethylene | [-] |
| PVC | Polyvinylchloride | [-] |
| SiC | Silicon Carbide | [-] |
| UV | Ultraviolet | [-] |
| μ_d | Dynamic coefficient of friction | [-] |
| μ_s | Static coefficient of friction | [-] |
| ΔL | Extension length | [mm] |
| σ | Vertical pressure force | [N] |
| τ | Tangential friction force | [N] |

TABLE OF FIGURES

| | |
|---|----|
| Fig. 1 types of friction welding process [9] | 12 |
| Fig. 2 diffusion of friction welding materials [28]..... | 13 |
| Fig. 3 Phases of friction welding process [29]..... | 14 |
| Fig. 4 friction welding parameters [30]..... | 15 |
| Fig. 5 real surface of two bodies [31] | 16 |
| Fig. 6 coefficient of friction [32] | 16 |
| Fig. 7 heat-affected area of arc methods [6] | 17 |
| Fig. 8 heat affected area of friction welding [6]..... | 17 |
| Fig. 9 Low temperature welding in Fe-Fe ₃ C diagram [16] | 18 |
| Fig. 10 Preparation and surface treatment [3]..... | 19 |
| Fig. 11 Weldability of materials [17]..... | 20 |
| Fig. 12 friction welded areas [33] | 21 |
| Fig. 13 Individual areas of friction weld [9] | 21 |
| Fig. 14 Cracks in friction welds [45] | 22 |
| Fig. 15 Friction welding machine [19]..... | 23 |
| Fig. 16 Pneumatic cylinder [34]..... | 24 |
| Fig. 17 Shaft [34] | 24 |
| Fig. 18 Exhaust turbine [34]..... | 24 |
| Fig. 19 Friction welded shaft [20]..... | 25 |
| Fig. 20 Friction welded gear [20]..... | 25 |
| Fig. 21 test specimens for tensile test [35]..... | 26 |
| Fig. 22 test specimen for Charpy impact test [36] | 26 |
| Fig. 23 bending test [37] | 26 |
| Fig. 24 Position of hardness test in welds [38] | 26 |
| Fig. 25 Carl Zeiss Stemi 508..... | 27 |
| Fig. 26 Olympus GX51 with camera Nikon DS-Fi | 27 |
| Fig. 27 Tensile test rod..... | 28 |
| Fig. 28 Scheme of hydraulic testing machine [39] | 28 |
| Fig. 29 Struers Secotom 60 | 29 |
| Fig. 30 Struers cutting disc..... | 29 |
| Fig. 31 Struers Citopress 15 | 29 |
| Fig. 32 Struers Tegramin 20..... | 30 |
| Fig. 33 Sanding papers | 30 |
| Fig. 34 Penetrative test [40] | 31 |
| Fig. 35 Magnetic powder test [41] | 31 |
| Fig. 36 Ultrasonic test [42]..... | 31 |
| Fig. 37 Rotation Jigs | 33 |
| Fig. 38 Static jigs | 33 |
| Fig. 39 camping of welded materials | 34 |
| Fig. 40 Contact of welded materials | 34 |
| Fig. 41 sparks in friction process | 34 |
| Fig. 42 forming suitable weld | 35 |
| Fig. 43 application of forging pressure | 35 |
| Fig. 44 Final weld | 35 |
| Fig. 45 AISI 316L final weld | 36 |
| Fig. 46 Ti GR2 final weld..... | 36 |
| Fig. 47 Macrostructure of AISI 316L | 37 |
| Fig. 48 Macrostructure of Ti GR2..... | 37 |
| Fig. 49 Microstructure of AISI 316L weld (10x zoom)..... | 38 |

| | |
|--|----|
| Fig. 50 Microstructure of Ti GR2 weld (10x zoom)..... | 38 |
| Fig. 51 Microstructure of AISI 316L and Ti GR2 weld (20x zoom)..... | 39 |
| Fig. 52 Microstructure of AISI 316L and Ti GR2 weld (150x zoom)..... | 39 |

TABLE OF FORMULAS

| | |
|---------------|----|
| (2.6.1) | 15 |
| (2.6.2) | 15 |
| (2.6.3) | 15 |
| (2.6.4) | 16 |

TABLE OF CHARTS

| | |
|---|----|
| Chart 1 Coefficients of friction of materials [3] | 16 |
| Chart 2 intervals of grinding for abrasive grain | 30 |
| Chart 3 Kroll solution | 30 |
| Chart 4 Marble solution | 30 |
| Chart 5 chemical composition of AISI 316L [25] | 32 |
| Chart 6 Chemical composition of TI GR2 [26] | 32 |
| Chart 7 values for samples without preheating | 40 |
| Chart 8 values for samples with preheating | 41 |

TABLE OF GRAPHS

| | |
|---|----|
| Graph 1 Tensile strength of samples without preheating..... | 40 |
| Graph 2 Maximum loading force of samples without preheating | 40 |
| Graph 3 Tensile strength of samples with preheating | 41 |
| Graph 4 Maximum loading force of samples without preheating | 41 |

TABLE OF ATTACHMENT

| | |
|---|--|
| Attachment 1 Information about hydraulic testing machine ZD40/400kN | |
| Attachment 2 Certificate of AISI 316L steel | |
| Attachment 3 Certificate of Ti GR 2 titanium | |
| Attachment 4 Microscopic photos of friction welds | |

Příloha č.1 Hydraulický zkušební stroj ZD40 /400kN/

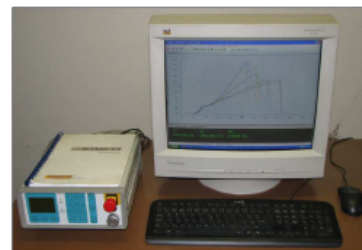
Stroj umožňuje provádět tahové, tlakové a ohybové zkoušky materiálů do 400 kN s řízením rychlosti zatěžování a programovým zpracováním zkoušek. Je vybaven vestavěným inkrementálním délkovým snímačem polohy příčnicku s rozlišením 0,01 mm a snímačem síly s řídicí jednotkou EDC 60.

Řídicí jednotka EDC 60 je vysoce precizní elektronické zařízení speciálně konstruované pro řízení servo-hydraulických zkušebních strojů. Je vyráběna speciálně pro aplikace řízení zkušebních strojů a využívají ji přední evropské výrobci universálních zkušebních strojů. Jednotka je opatřena programem pro zkoušky kovů s možností provádět zkoušky bez PC u jednoduchých aplikací bez použití průtahoměru.


Technické parametry:

- Výrobce: HBM /SRN/
- Měřicí rozsah: 8 ÷ 400 kN
- Chyba měření síly: 1/100 jmenovitého rozsahu síly, tj. $\pm 1 \%$ odpovídá třídě přesnosti 1
- Měřicí rozsah měření dráhy: 0 ÷ 280 mm
- Chyba měření dráhy: $\pm 0,01$ mm
- sériové rozhraní RS 232 pro komunikaci s nadřazeným PC
- COM1 pro PC s FIFO s maximální rychlostí 115 KB
- inkrementální vstup pro napojení snímače dráhy

Počítač je vybaven programem M-TEST v.1.7 pro tahovou, tlakovou a ohybovou zkoušku kovových materiálů dle EN 10001-2 s vyhodnocením výsledků, grafickým zpracováním.



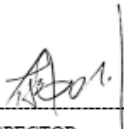
Řídicí jednotka EDC 60

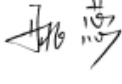
 **TITANIUM LASTING**

SHAANXI LASTING TITANIUM INDUSTRY CO., LTD.
 Add:1#, Zhuque Road,Xi'an, Shaanxi, China 710061 EN9120:2018 CERT NO. :4235000

QUALITY CERTIFICATE Acc. to EN10204/3.1+PED 2014/68/EU
 NO: HP8296-T-4 DATE: Jun.13,2019

| | | | | | | | | |
|--|----------------------------|----------------|--------------------------------------|--|--------------------|--------------------------|---------------------|---------|
| Commodity : Titanium Round Bar Gr.2 | | | | | | Finish: Annealed | | |
| Specification :Acc. to ASTM B348-13, ASME SB348-13,ASTM F67,NACE MR0175/15156-1. | | | | | | | | |
| Size | | Quantity (pcs) | Net Weight (kgs) | Heat No. | Lot No. | | | |
| Dia20(h9:-0.052/+0) x L3000-3100mm Straightness ≤ 1mm/1m | | 126 | 550.00 | 2019-2 | / | | | |
| Chemical Composition (wt.%) | | | | | | | | |
| Requirement (MAX) | FE | C | N | H | O | Residuals Each | Residuals Total | TI |
| | 0.30 | 0.08 | 0.03 | 0.015 | 0.25 | 0.10 | 0.40 | Balance |
| Result | 0.20 | 0.011 | 0.012 | <0.0006 | 0.144 | <0.10 | <0.40 | Balance |
| Tensile Test | | | | | | | | |
| Requirement | Tensile Strength (MPa) min | | Yield Strength,0.2% Offset (MPa) min | | Elongation (%) min | Reduct. of area (%) min. | | |
| | 345 | | 275 | | 20 | 30 | | |
| Result | 497 | | 332 | | 35 | 57 | | |
| Other Test | | | | | | | | |
| Dimensional Inspection | Visual Inspection | | | Ultrasonic Inspection Acc. To AMS 2631 D Class A1 | | | Hardness Test (HRB) | |
| Acceptable | Acceptable | | | Acceptable | | | 84 | |
| We hereby certify that the material described above has been tested/analysed and conform to complies with the terms terms as per purchase order No.HP8296 Date April.16,2019 confirmation Inspection and dimensional control without complaints. | | | | | | | | |


 INSPECTOR


 AUDITOR


 MANAGER OF QUALITY DEPARTMENT

AISI 316L friction welds

